Spring 1983

Control of rock fragmentation through explosive coupling

Timothy Wayne Warden

Department:

CONTROL OF ROCK FRAGMENTATION THROUGH EXPLOSIVE COUPLING

BY

TIMOTHY WAYNE WARDEN, 1959-

A THESIS

Presented to the Faculty of the Graduate School of the

UNIVERSITY OF MISSOURI-ROLLA

In Partial Fulfillment of the Requirements for the Degree

MASTER OF SCIENCE IN MINING ENGINEERING

1983

Approved by

(Advisor) Charles J. Haas

ABSTRACT

Both detonation pressure and borehole pressure, resulting from an explosion within blastholes in rock, perform specific functions in the fragmentation of the rock and the generation of ground vibrations. The results of previous investigations would suggest that control of these pressures in the borehole would, to some extent, control the size distribution of the blasted particles. One method of influencing detonation and borehole pressures is by varying the hole diameter in relation to a constant charge diameter, called decoupling, and by varying the medium between the explosive charge and the rock.

This investigation examined the effects of geometric coupling, which is the ratio of the charge diameter to the hole diameter, using water and air coupling mediums, on the degree of fragmentation. A total of eleven reduced-scale in situ bench blasts were performed, and the broken rock resulting from each blast was screened into eight size-fractions. These size-fractions were grouped into coarse, medium, and fine size ranges in accordance with a scaling factor ranging between 10 and 15.

The results indicated that a linear relationship exists between geometric coupling and the corresponding cumulative weight percentages in each size range for both air and water coupling. Percentages of material in all size ranges, particularly the coarse and medium, can be controlled to some extent by geometric coupling ratios and the coupling medium. In general, water coupling produced greater degrees of fragmentation and lower magnitudes of peak particle velocity than did air coupling.

ACKNOWLEDGMENTS

The author wishes to express his indebtness and sincere appreciation to his principal advisor, Dr. Norman S. Smith for his continued guidance and constructive criticism throughout this investigation and to Dr. Charles Haas and Dr. Nolan B. Aughenbaugh for their valued criticisms and ideas in the preparation of this thesis.

Thanks and appreciation are extended to Dave Ausmus and Joe Brinkmann for their interest and invaluable assistance with the field work, and to Everett Bleakney III, Troy Harris, and James Smith who also provided help on the experimental phase of this work.

The writer is indebted to the Department of Mining Engineering and the Chancellor's Fellowship Committee of the University of Missouri-Rolla, the Ensign Bickford Company, and the Henry Dewitt Smith Memorial Endowment Fund of the American Institute of Mining, Metallurgical and Petroleum Engineers, for their financial support throughout his graduate studies.

Special thanks are extended to the author's mother and father for whom this thesis is dedicated.

TABLE OF CONTENTS

Table of Contents (cont'd) Page

Table of Contents (cont'd) Page

LIST OF ILLUSTRATIONS

List of Illustrations (cont'd)

List of Illustrations (cont'd)

List of Illustrations (cont'd)

Figure Page

LIST OF TABLES

I. INTRODUCTION

The actual process involved in rock breakage by explosives is extremely complex, and is not completely understood. It is a generally accepted fact, however, that when an explosive is detonated within a borehole, two pressures are generated - detonation pressure and explosion pressure. Each of these pressures contribute to the fragmentation of the rock and to the side effects of each blast.

"Detonation results when there is a supersonic shock wave propagated through the explosive that is accompanied by a chemical reaction that furnishes energy to sustain the shock wave propagation in a stable manner," (Ash, 1973). The value of detonation pressure is approximately equal to the product of the explosive density and the square of the detonation velocity. Since the detonation front acts on a very small portion of the borehole wall at any instant of time, the detonation pressure associated with this front is transient and relatively short-lived. The effect of detonation pressure on the rock is characterized by shock waves, local crushing around the borehole perimeter, and initiation of radial cracks at preferential locations. The magnitude of detonation pressure for a given explosive, and its action on the surrounding rock, is dependent upon the priming system, degree of charge confinement, charge diameter, and loading density.

Explosion pressure is a quasi-static pressure resulting from adiabatic expansion of the explosive gases subsequent to detonation. Its value is approximately equal to one-half that of the ideal detonation pressure for that particular explosive, assuming the gases as being confined to the original volume of the explosive charge. Although this assumption is valid for conditions with bulk-loaded explosives in a

borehole, it does not translate to the actual pressure experienced on the walls of the borehole when the diameter of the explosive charge is less than that of the borehole. Under this condition, the effective borehole pressure, due to gas expansion, will be less in value than the calculated explosion pressure. Explosion pressure, therefore, is only dependent upon the nature of the explosive, while the effective borehole pressure is influenced also by the actual loading conditions. Both are considered by many to be responsible for radial crack extension and the final state of rock fragmentation by flexure or some other mechanism.

A. FRAGMENTATION

Fragmentation is a term used in various ways to describe the relative size distribution of the broken rock resulting from a blast. The importance of controlled fragmentation is highly emphasized, since the overall efficiency of an operation may be dependent on the performance of the blast. The degree of fragmentation is commonly used to describe the degree of fineness of the blasted rock. In most cases fineness is a indicator of efficiency for blast performance; however, in some situations fineness of the rock may not be the goal of the operation. There are instances when a uniform coarse product is desired.

The relationship of explosion-generated pressures to the degree of fragmentation is generally recognized as one of major importance. Particular explosives may be selected for rock blasting on the basis of their rated pressures. The magnitude of these rated detonation and explosion pressures provided a viable means for comparing various

explosives. They do not, however, offer the complete solution for controlling the degree of fragmentation, since the actual pressures experienced within the borehole are influenced by the extent of decoupling, and the relationship between decoupling and fragmentation is not fully understood.

B. GROUND VIBRATION

The energy released from the detonation of an explosive is only partially directed toward fragmentation. An estimated 2-20% of the energy released by the explosion process is partitioned to seismic wave formation. Controversy exists as to whether the source of this side-effect is detonation pressure, explosion pressure, or both.

Seismic waves are of two types - body waves and surface waves. Body waves in rock will generate surface waves when they strike a free surface bounded by air or water. Surface waves are of significance in rock blasting because of their potential for causing environmental disturbance and damage. The measurable unit of surface waves is particle velocity, which is the critereon upon which regulatory limits are based. There are indications that an inverse relationship exists between the magnitude of peak particle velocity and the degree of fragmentation.

C. EXPLOSIVE DECOUPLING

Explosive decoupling is a term which indicates a state of physical separation of an explosive charge from a rock surface, usually the wall of the borehole. For instance, a decoupled situation exists when the diameter of a cylindrical explosive charge is less than the diameter of the blasthole. The result of decoupling is a reduction in the magnitude of the explosive-generated pressures experienced on the wall of the borehole, and a subsequent reduction in the amount of energy transmitted

into the rock mass.

Since detonation pressure is influenced by the degree of confinement, it follows that decoupling will reduce the magnitude of the detonation pressure. In addition, the effective borehole pressure on the walls of the borehole will be reduced below that of the explosion pressure because of the excess volume available for gas expansion. This combined loss in efficiency of explosive energy transfer to the rock would suggest a cause for a lower degree of fragmentation of the rock and a reduction in the level of ground vibrations. However, this rational conclusion may be over simplified.

D. THE PROBLEM

There are two considerations associated with explosive decoupling: the spacial separation of the explosive and the rock, and the nature of the medium that separates the explosive and the rock. Both aspects have been related to blasting efficiency in terms of strain energy development in the rock or extrapolations to the degree of fragmentation. No relationship exists between explosive decoupling, involving both space and medium, and a complete fragmentation analysis of the blasted rock. Furthermore, there are indications that explosive decoupling may not result in a lower degreeof fragmentation, at least for all spacial relationships and all decoupling mediums, when all the particle-size ranges are examined.

The hypothesis of this investigation is that explosive decoupling has the potential of controlling, to some extent, the overall of fragmentation from a blast, and particularly, that of either the coarse or fine size ranges. The experimental method used to examine this hypothesis involved reduced-scale in situ bench blasts, complete screen

analyses of fragments, air and water decoupling mediums, and various decoupling ratios. Ground vibrations were measured and recorded for all tests.

II. REVIEW OF LITERATURE

A. FRAGMENTATION ASSESSMENT

The collection and interpretation of data obtained for the purpose of defining the overall particle size distribution, resulting from a blast, is referred to as fragmentation assessment. The method of acquisition of this data is partially dependent on the relative size of the blast: full-scale operational blasts, small-scale laboratory blasts, or reduced-scale in situ blasts.

The cost for a complete screen size analysis for a full-scale operational blast is extremely excessive. Consequently, investigators have used random sampling or some remote methods for collecting fragmentation data. Three procedures frequently used are: random sampling of the blasted rock, the "boulder" count technique, and photographic analysis. Although, these techniques are designed primarily for use in full-scale blasts only, the "boulder" count technique has been utilized in some reduced-scale in situ blasting experiments, particularly by Persson et. al., (1969) and Keller, (1982). A detailed description of the full-scale fragmentation assessment methods are presented by Just, (1979), and Brinkmann, (1982).

Small-scale blasting studies performed by Da Gama, (1971, 1974), Bhandari and Vutukiri, (1974), and Bhandari, (1975) measured the complete size distribution of blasted rock and used mineral processing methods to evaluate the data. Bhandari and Vutukiri examined the effects of geometric coupling ratios on fragmentation from bench blasting in small blocks of mortar. The results were presented in terms of fragment weights and photographs for visual comparison. Da Gama used small scale bench blasts in limestone and granite to

evaluate the concept of blasting as a comminution process in order to understand the energy-size reduction relationships for various blast design patterns. Da Gama recovered all the blasted rock, and screened every particle. A general size-distribution law was obtained by plotting the cumulative undersize weight percent versus the dimensionless ratio between particle size and burden, on log-log graphs. The main drawbacks of such small scale experiments are the difficulties in extrapolating the results to full scale, since the experiments are usually conducted in materials other than rock, such as Plexiglass or mortar.

Bergmann et. al., (1973) experimented on a slightly larger scale using large homogeneous blocks of granite weighing in excess of fifteen tons. Bergmann performed a complete screen size analysis on all the blasted rock, representing the degree of fragmentation by a single index-- the average fragment size. The average fragment size was obtained by identifying the screen size on the mineral processing curve which passes 50 percent of the material.

For acceptable extrapolation of experimental results to full scale the material blasted should have a heterogeneous character. Reduced-scale is sufficiently close enough to full scale to be representative, yet allowing complete fragment recovery and size-distribution. Also, the type of explosive used and the experimental blast design should be representative of full-scale operational blasts. Such conditions can be obtained by using reduced-scale in situ bench blasts. Ash, (1973), Dick et. al., (1973), Smith, (1976), and Brinkmann, (1982) have used this technique to evaluate the degree of fragmentation from various blast design relationships.

Dick et. al., retained all the blasted fragments, and performed a complete screen analysis to determine the relative size distribution for each bench blast. Mineral processing applications were used to measure the uniformity and the extent of fragmentation, relative to the slope and intercepts obtained from the log-log plot of the size distribution line.

Smith and Brinkmann related various fragmentation indices to the overall degree of fragmentation for each blast. A series of bar charts were constructed to show the percent of material passing various screen sizes. A 50-percent-passing line was established on the bar chart; this was comparable to the average particle size used by Bergmann, (1973).

B. GROUND VIBRATION

When an explosive is detonated inside of a borehole the pressures generated produce intense shock waves in the rock. "Some of the energy released by the explosion destroys the coherency of the immediate rock, while the remaining shock energy passes into the rock as a compressional shock front traveling at a Velocity slightly higher than the sonic velocity of rock, "(Attwell, 1964). A short distance from the blast this velocity will be reduced to the sonic velocity of the rock, the intensity of the stress wave decreases, and it becomes stable. These stable waves produce no permanent deformation in the rock mass as it passes, and are called elastic waves. The two waves of importance in blasting are body waves and surface waves. Body waves travel through the interior of the rock while surface waves travel along its free surface or interface of air or water. There are two types of body waves, dilatational and distortional. Dilitational waves, also referred

to as longitudinal, P-waves, compressional or sonic waves, are characterized by having particle motion in the direction of propogaton. Distortional waves, also referred to as shear waves, or S-waves have particle motion perpendicular to the direction of travel. When a body wave strikes a boundary, surface waves are formed. The best known and most easily detected surface waves are called Raleigh waves, and the disturbances associated with them decay exponentially with depth from the surface and distance from the blast. "Since these waves spread only in two dimensions, they fall off more slowly with the distance than the other types of elastic waves," (Kolsky, 1952). Surface waves are evironmentally important when blasting. Surface structures are susceptible to damage from these waves if certain levels of magnitude are exceeded, and a nuisance factor may be realized with lower levels of ground vibrations.

1. Factors Influencing Ground Vibration Magnitudes. Currently the most widely accepted standard of measurement of ground motion resulting from blasting is the magnitude of the particle velocity, Particle Velocity is the rate of motion for individual particles at a point caused by the surface waves passing that particular point. damage to surface structures can be related to various magnitudes of particle velocity. This has prompted Federal and State regulatory agencies to set maximum limits on peak particle velocity for ground vibrations imposed on the public by blasting operations. A relationship between peak particle velocity and scaled-distance has been developed by the United States Bureau of Mines for estimation of ground motion. The relationship is defined as follows:

$$V = 160\ (R/W^{\frac{1}{2}})^{-1.60}$$

Where: V = peak particle velocity of all three orthogonal components at a point, inches per second;

R = distance from blast to the given point, feet;

W = maximum charge weight in the blast per delay of at least 8 milliseconds, lb.; and

$R/W^{\frac{1}{2}}$ = scaled distance, $ft/lb^{\frac{1}{2}}$

DuPont, (1977) relates scaled distance to peak particle velocity for various levels of confinement. Some methods of controlling ground vibration levels through the blast design are listed in DuPont, (1977). Seismic waves characteristically decrease in magnitude with distance from the shotpoint. At these larger distances low frequency waves are more predominant than high frequency waves. The extent of predominance is influenced by the rock type, since high frequency seismic energy is absorbed more readily than low frequency seismic energy. Recent developments by Taqieddin, (1982) indicate that the location of the explosive primer in the blasthole influences ground vibration magnitudes. In essence, collar priming produces significantly higher magnitudes of peak particle velocity than does bottom priming. Proper coupling of the geophone to the ground, and the internal accuracy of the recording instrument also influence the measured values of the peak particle velocity.

2. Ground Vibration Assessment. The device used for measuring and recording seismic data is called a seismograph. The three main types of recording instruments are the displacement, velocity, and acceleration seismographs. The velocity seismographs measure the particle velocity of the seismic waves at a particular location, and are

the most commonly used type in blasting. The most important element of any seismograph is the transducer, which is contained in the geophone unit. A transducer responds to motion in one of three orthogonal directions; longitudinal, vertical, or transverse components. A four channel system indicates that the seismograph has one transducer measuring each of the three orthogonal components, and one external channel measuring the air over-pressure. The geophone must always be satisfactorily coupled to the ground, and oriented so the longitudinal component is directed toward the blast. Blasting seismographs are normally constructed to measure particle velocities ranging from about 0.1 to 10 inches per second over a frequency range of 2 to 200 Hertz (DuPont, 1977). Most seismographs record the seismic disturbance on a magnetic tape, and show the magnitude of the peak particle velocity on a meter. A printed wave form of the blast can be obtained by processing the magnetic tape.

C. EXPLOSIVE DECOUPLING

Explosive decoupling is defined by the existence of an annulus between an explosive charge and the wall of the borehole. The material filling the annulus is called the coupling medium, even though it is associated with a state of decoupling. The dimensional aspect of explosive decoupling is referred to as geometric coupling, which is defined as the ratio of the diameter of the cylindrical explosive, D_c, to the diameter of the blasthole, D_h. Geometric coupling is used as the independent variable in a number of blasting research projects.

In the early 1960's the United States Bureau of Mines began an extensive series of field tests, to determine the effect of the ratio of characteristic impedances, of the explosive and the rock, on the

levels of energy transmitted into the rock mass. Characteristic impedance is defined for the explosive as the product of mass density and detonation velocity; for the rock it is defined as the product of mass density and sonic velocity. The level of energy transmitted to the rock mass was defined by the magnitude of strain waves. "The wave motion associated with an explosive impact is considered essentially a form of particle displacement, and strain propogation is attributed to the vibratory nature of this displacement," (Quan, 1964). The United States Bureau of Mines determined that a characteristic impedance ratio equal to unity produced the highest strain wave amplitudes in the rock. Nicholls, (1962) followed with a similar study, determining the explosive energy transferred into the rock for four geometric coupling ratios, using air as the coupling medium. He concluded that as the geometric coupling ratio, D_c/D_h, decreased, the strain wave amplitude decreased, therefore, less energy was transferred into the rock mass.

Recently, much interest has been directed to the efficient use of explosive energy, particularly in regards to the effects of explosive decoupling on rock fragmentation. "The amount of wasteful crushing and superfragmentation can be reduced, or eliminated altogether, by decoupling (i.e. by providing an annulus of air between the charge and the blasthole wall)." (Hagan, 1979). Hagan also states that a decoupled explosive produces better effective fragmentation and rock movement, with muckpiles showing characteristics comparable to those for larger blasthole patterns. Effective fragmentation, although not defined by Hagan, imples a decrease in the undesirable oversize and undersize

fragments, while increasing the quanity of desirable middle size fragments. The definition of a desirable product will vary depending on the operation. There is some evidence that decoupling an explosive with air alters the rock breakage process, however, a comprehensive fragmentation analysis to support this evidence is not presently available.

1. Influence of Air Coupling on Explosive Performance. When an explosive is decoupled two important physical changes occur within the borehole; a reduction in explosive confinement, and the creation of a volume for gas expansion which is in excess of the original explosive volume. The reduction in confinement, to a degree, reduces the detonation pressure. The explosion pressure is usually defined as the magnitude of the hydrostatic pressure reached after all the explosion products have acquired thermal and chemical equilibrium in the volume initially occupied by the explosive, and is usually considered to equal one-half the detonation pressure for an ideal state of full detonation. "For all practical purposes the borehole (explosion) pressure would be dependent only on the explosive's chemical composition, density, initial volume, and on the conditions that a complete reaction and no change in volume occur," (Ash, 1973). For conditions where a change in volume does occur because of geometric decoupling, Ash suggests the following relationship between explosion pressure, geometric coupling, and effective borehole pressure:

$$P_b = P_e (D)^2$$

Where: P_b = Effective borehole pressure, psi;

P_e = Ideal explosion pressure, psi; and

D = geometric coupling, D_c/D_h.

Bergmann, (1973) conducted a series of experiments in large blocks of homogeneous granite. A single explosive charge of constant diameter, density, and weight,was used to determine the influence of geometric coupling on fragmentation. Control of the hole diameter enabled a variable range of geometric coupling ratios, without the necessity of considering the effect of changes in multitudes of other associated blast parameters. Bergmann determined an empirical relationship between effective borehole pressure, and geometric coupling, which is defined below:

$$P_b = P_{det} \times D^{1.90}$$

Where: P_b = effective borehole pressure, psi;

P_{det} = detonation pressure, psi; and

D = geometric coupling, D_c/D_h.

A complete screen analysis of the blast fragments indicated a direct linear relationship between fragmentation and effective borehole pressure.

Ucar, (1975) decoupled a cylindrical explosive charge and found that the effective borehole pressure, P , varied as a function of explosion pressure, Pe, and the geometric coupling ratio, D, by the following relationship:

$$P_b = P_e \ (D)^5$$

This equation was originally derived by Cook, (1958) empirically, using several explosives at various loading densities and, as reported by Ucar provides a relatively good approximation of the borehole pressure for decoupling ratios greater than 0.60.

Considerable differences are noted between the equations derived

by Ash, Bergmann, and Cook for determining the effective borehole pressure when the explosive is decoupled.

Persson et. al., (1968) performed reduced-scale in situ bench blasts in a homogeneous granite formation to examine the rock blasting capability of a single cylindrical explosive charge, using four geometric coupling ratios. A constant diameter cap-sensitive explosive was loaded into plastic tubes, and decoupled with air by drilling four sequentially larger diameter blastholes. Upon examination of the crater volume and the burden velocity, it was apparent that a geometric coupling ratio of about 0.50 gave optimum results. "In the optimum hole diameter, the charge thus not only breaks away a severalfold greater mass of rock but also throws this greater mass a longer distance than it does in a smaller or larger diameter hole," (Persson, 1968). A greater utilization of the explosive energy is obtained at the optimum D_c/D_h value, however, this energy is not directed toward rock fragmentation, but rather toward crater formation and heaving of the rock. Fragmentation was examined, but a complete screen analysis was not performed. It was assessed by a version of the "boulder" count technique, whereby the nine largest boulders resulting from each blast were weighed. Using this technique to evaluate fragmentation does not, however, describe the overall degree of fragmentation, but merely quantifies the oversize fragments, occurring at that geometric coupling ratio.
It should also be noted that all experimental work dealing with decoupling, with the exception of Nicholls, (1962), used the hole diameter as the means to vary the decoupling ratio, thereby avoiding the design complications associated with a changing explosive diameter.

Numerous investigators have suggested that a more effective distribution of the explosive energy could be realized with a decoupled explosive. Hagan, (1979) states that reduction of the percentage of fines can be accomplished by decreasing the geometric coupling ratio. This has importance since excessive fines can result in an unrecoverable mineral loss when certain ores are being mined, and may even increase processing costs. In most situations, as with normal quarry blasting, the production of excessive fines has little bearing on mining profitability; however in some cases fines in blasted material cause problems. Prevention of excessive crushing in the immediate vicinity of the borehole may offer other advantages, aside from reducing fines. "Crushing of the rock near the explosive charge contributes very little to the total fragmentation, but causes very high rates of dissipation of strain wave energy," (Hagan, 1974). A reduction in the energy dissipation rates could improve the overall explosive efficiency. "Although there is some evidence [Hagan, (1973); Persson et. al., (1968); Melnikov, (1962)], that prevention of crushing, by decoupling, may improve performance, more extensive experimentation is required," (Hagan, 1974).

Melnikov, (1962) reported that the use of air gaps to separate charges in the explosive column promotes more efficient utilization of the explosive energy and better "blasting results." The function of the air gaps is to reduce the pressures of the explosion, and increase the duration of their action on the rock. Melnikov recommended an optimum borehole-volume-to-explosive-volume ratio between two and three. For illustrative purposes this optimum volume ratio, equated in terms of geometric coupling ratios, ranges from from 0.71 to 0.58.

Johansson et. al., (1974) discussed the method of decoupling using wooden spacers between the charges, by distributing the explosive throughout 40 percent of the upper portion of the hole volume. This form of decoupling is also said to reduce the energy losses associated with the shock wave. "The subsequent isentropic expansion will then start with undiminshed energy content of the gas but at a lower pressure," (Johannsson and Persson, 1970).

2. Influence of Water Coupling on Explosive Performance. "The effect on geometric coupling of an annular ring of fluid, soil or sand surrounding the charge has not been investigated," (Nicholls, 1962). The experiments performed by Nicholls, (1962); Fogelson, (1968); Persson, (1968); and Bergmann, (1973) involved air as the coupling medium. In an actual operational blasting situation, however, the coupling medium may not be restricted to air. Commonly, water may infiltrate the borehole, thus changing the medium through which the dynamic pulse, caused by the detonation pressure of the explosive, is transferred into the rock. The magnitude of this dynamic pulse affects the depth of the crushed region in the immediate rock. Hagan, (1979) has expressed concern that both the geometric coupling ratio and the type of coupling medium influence the depth of this crushed region, and must be used to control it. Worsey, (1981), examined the relative effects of air-and water-coupled explosives on radial fracture extension in plexiglass blocks. Worsey found that the water-coupled PETN charges produced considerably more damage to the plexiglass than the air-coupled blasts.

Haas, (1964) measured the attenuation rates and the peak stress in a Yule marble block, using water, marble, sand, cardboard, air, and

other dissimilar materials for the coupling medium. "Layers of dissimilar materials placed between the explosive and the marble surface may increase or decrease the shock intensity, depending on what material is used." (Haas, 1964). The attenuation rate for water is the lowest of all the materials used by Haas, including the marble itself. The attenuation rate for air was the greatest. The peak stress was greatest for water, and lowest for air.

D. REDUCED-SCALE IN SITU MODELS

Reduced-scale in situ bench blasts offer several advantages over other methods of testing when fragmentation and its associated side effects are being examined. The following advantages led to the selection of this testing method for the current study. If proper requisites are fulfilled in designing the model, the fragmentation and other blast results can be related directly to full-scale operational blasts. The in situ model permits the influence of the heterogeneous characters of the rock on blast results, and the reduced-scale allows collection and screen analyses of all the blast fragments.

Persson et. al., (1968); Ash, (1973); Smith, (1976); and Brinkmann, (1982), have used this in situ modeling technique to investigate the influence of blast design variables on fragmentation. Persson, however, used a single explosive charge in homogeneous rock, and chose not to evaluate fragmentation by screen analyses. Smith, (1979, 1980) and Taqieddin, (1982) also used this technique to study ground vibrations from blasting.

Ash, (1973) and Dick et. al., (1973) performed a combined total of 20 reduced-scale bench blasts at a dolomitic limestone quarry in Stewartville, Minnesota. Ash conducted 12 tests to determine the

effects of geologic structural discontinuities on rock blasting and find a suitable criteria upon which to relate the effect of their presence on the design of blasts in mining and heavy construction. Dick used eight bench blasts to study the effects of the site, timing of initiation, and burden-to-spacing ratio on the degree of fragmentation.

Smith and Brinkmann conducted a combined total of 33 reduced scale bench blasts at a dolomitic limestone quarry in Rolla, Missouri. Smith determined the relationship between burden rock stiffness and the degree of fragmentation resulting from 20 bottom primed test blasts. Brinkmann repeated Smith's tests to determine the effect of collar priming on fragmentation and ground vibrations. The fragmentation data obtained from Smith; (1976), and ground vibration data from Smith, (1979, 1980) tests, allowed Brinkmann to have a direct comparison between bottom-primed and collar-primed results.

1. Considerations for Model Design. When designing an in situ model, certain requirements must be met. Ash, (1973) has suggested a set of qualifications to follow when developing a reduced-scale in situ bench blasting model:

1. Explosive charges should be cylindrical with a length of at least twenty times their diameter.
2. The explosive used must have properties that closely approximate normal industrial products.
3. Equipment and labor requirements should be at a minimum for testing.
4. The rock formation should be anisotropic, bedded, jointed, and reasonably competent.

5. Blasted rock fragments must be recoverable for screen analysis.

6. Craters formed and geologic discontinuites should be easily definable.

The experimental in-situ bench blasting investigations discussed previously, with the exception of Persson, (1968), used a blast design with a three hole configuration. This enabled manipulation of the geometric relationships in the design, while providing each explosive charge with three free faces for blasting. Closely controlled models of this type very acurately depict the prototype, which is necessary in order to extrapolate the results to full scale.

2. Relationship to Full-Scale. The relationship of the dimensions of a model to that of the prototype is referred to as geometric similitude. Dimensional analysis is the common approach to understanding similitude, since the coefficient of the linear dimension determines the coefficient of the scaling factor. The individual linear dimensions of a reduced-scale in situ model can be related to the prototype as follows:

$$d_p = K\, d_m$$

$$B_p = K\, B_m$$

$$S_p = K\, S_m$$

$$L_p = K\, L_m$$

Where d, B, S, L are the hole diameter, burden, spacing, and bench height respectively, p and m denote the prototype and the model; and K is the selected scaling factor. The percentages and dimensionless fragmentation indices used in previous works to describe the degree of fragmentation remain unchanged from model to prototype. Areas and volumes are related, from model to prototype, by K^2 and K^3 respectively.

Other important considerations in the design of reduced-scale bench blasting models involve dynamic similitude. Basically this relationship can be summarized as one involving mass, stress, energy, and elastic properties. The entire process of relating these quantities from the model to the prototype is quite complicated. A simplification of the variables is possible, however, if the properties listed above for the rock mass and the explosive are the same for the model and the prototype. An excellent explanation of dynamic similitude for models and prototypes with similar properties, and those with different properties, is presented by Da Gama, (1970).

III. EXPERIMENTAL PROCEDURE

The purpose of this investigation was to examine the effects of geometric coupling ratios and coupling mediums on the degree of fragmentation and the magnitude of ground vibrations resulting from bench blasting in dolomite rock. The experimental program consisted of eleven reduced-scale in situ bench blasts, using seven geometric coupling ratios and two coupling mediums. The geometric coupling, D_c/D_h, ranged from 0.15 to 1.00; the coupling mediums were air and water for the decoupled tests, and one blast was a fully coupled test. Ground vibrations were recorded for each blast at a constant scaled distance of 21.3 $ft/lb^{\frac{1}{2}}$, and the resulting fragmentation screened in its entirety.

The test blasts were performed in the Jefferson City dolomite formation at the quarry of the University of Missouri-Rolla Experimental Mine. This quarry is located on the southwestern edge of Rolla, in Phelps County, Missouri.

The elastic properties of the Jefferson City dolomite formation are given in Appendix A.

Reduced-scale in situ bench blasts have previously been conducted on this site for fragmentation and ground vibration experimentation, and the procedures have been well established. The current study used a three-hole single-row pattern for all tests, and the holes were oriented perpendicular to the dominant geologic joint sets. An illustration of the idealized blast design used for this study is shown in Figure 1. The explosive charge length, weight and diameter remained constant for all test blasts, and the geometric coupling was controlled

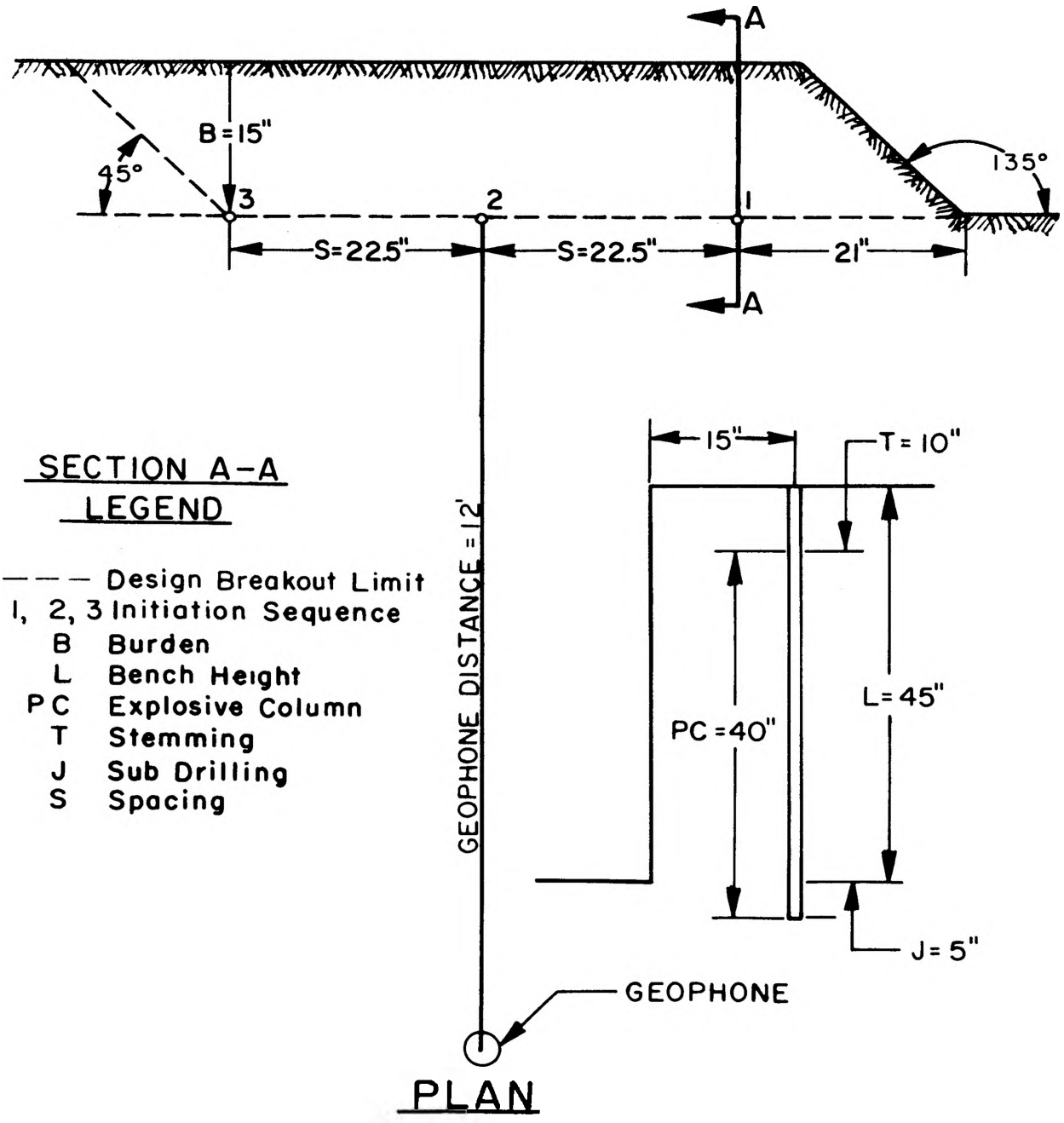

Figure 1. Idealized Design for Test Blasts.

by drilling various diameter blastholes. Properties of the explosive used in this study are outlined in Table A-II. Each test blast for this study was identified by the letters W, A, or F, to denote water coupling, air coupling, and full coupling, respectively. The numbers succeeding the letters denote the geometric coupling ratio times 100. For example test blast W-57 indicates a water-coupled explosive with a geometric coupling of 0.57. The explosive charge geometry and loading condition for each test blast are outlined in Table I.

A. BENCH PREPARATION AND MAPPING

A vast majority of the physical effort required for this study was in the preparation of the vertical bench for each test blast. The objective of bench preparation was to obtain a straight vertical face matching the design configuration in Figure 1 as close as possible. Smooth-wall blasting, hand chiseling, and chipping with an air-powered paving breaker were the means used to construct the designed bench configuration.

The equipment and general procedures used for mapping were obtained from Keller, (1982), and modified slightly for use in this investigation. Each test blast was mapped before and after blasting to obtain face contours for volume and weight calculations of endbreak, backbreak, toe, and the total crater size. Photographs, burden rock contour maps, and cross-sections for each test blast are shown in Figures E-1 through E-33.

For mapping purposes a permanent reference line was established by placing several nails near the bench face along a straight line on the quarry floor. A reference screen was positioned along this line,

TABLE I

EXPLOSIVE CHARGE GEOMETRY AND LOADING CONDITIONS*

Blast No.	Hole Diameter D_h, inches	Geometric Coupling D_c/D_h	Coupling Medium
F-1	0.50	1.00	Rock
A-57	0.88	0.57	Air
A-47	1.06	0.47	Air
A-40	1.25	0.40	Air
A-33	1.50	0.33	Air
A-48	1.75	0.28	Air
W-57	0.88	0.57	Water
**W-47	1.06	0.47	Water
W-40	1.25	0.40	Water
W-33	1.50	0.33	Water
W-28	1.75	0.28	Water
W-15	3.25	0.15	Water

*Charge diameter = 0.50-inches, length = 40-inches, lbs/delay = 0.317, and specific gravity = 1.12, remained constant for all test blasts.

**Smith shot S-32, (1980).

aligned with a carpenter's level, and held in place with small timbers. Figures 2 and 3 show procedure for mapping with the reference screen in position. Distances from the bench face to the reference screen were measured at 4-inch intervals by sliding a 0.38-inch steel graduated rod through the 0.50-inch wire mesh.

B. FRAGMENT RETENTION

Since the objective of this study was to determine the degree of fragmentation for the entire mass of blasted rock, maximum fragment recovery with minimum contamination was necessary. The quarry floor and immediate area were swept and then blown clean with compressed air, and sheets of polyethylene were laid out in the immediate test area to capture any flyrock escaping the test pit. A blasting mat was constructucted by loosely placing wire mesh against the bench face, and leaning oak timbers over, but covering the bench. In nearly every case the blasted rock was retained within the test pit, and little flyrock was observed. Figures 4 and 5 show a typical blast before and during blasting; Figures 6 and 7 show a blast immediately after blasting, and immediately before weighing.

C. SEISMOGRAPH POSITIONING

Prior to the initiation of this investigation several tests were performed with a blasting seismograph to develop procedures for obtaining comparative ground vibration results. Ground vibrations were monitored for several reduced-scale single hole crater blasts, which revealed the following:

1. A sandbag weight of 50 pounds on the geophone provided adequate weight for consistent ground vibration results.

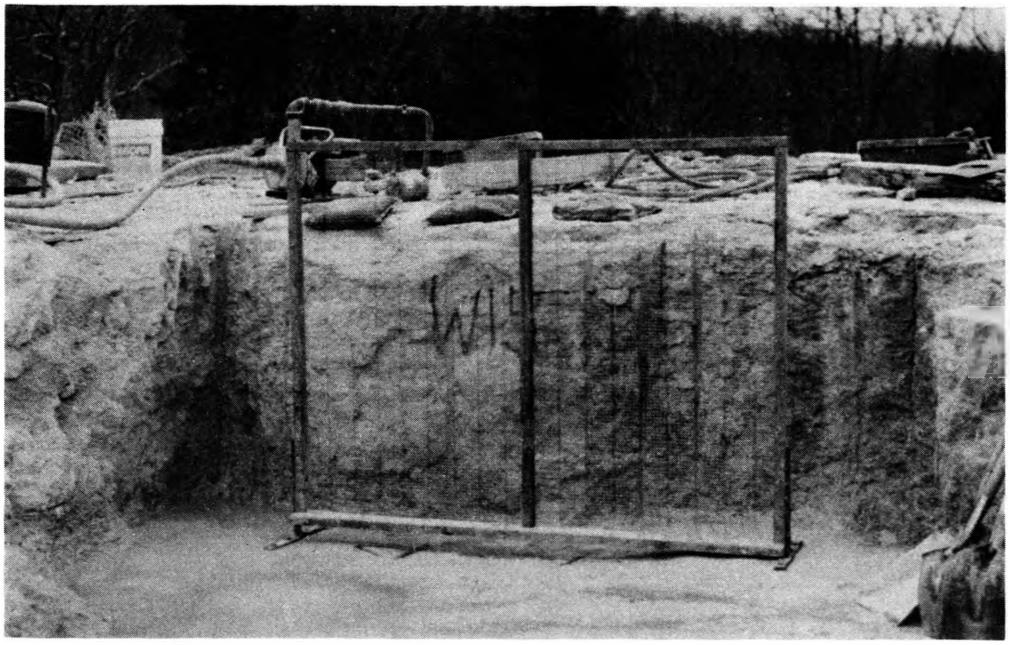

Figure 2. Mapping Screen in Position.

Figure 3. Procedure for Face Mapping.

Figure 4. Typical Test Site Before Blasting.

Figure 5. Typical Test Shot During Blasting.

Figure 6. Typical Test Site Immediately After Blasting.

Figure 7. Typical Test Site Immediately Before Screening.

2. Incompetent rock directly beneath the geophone caused an increase in the recorded ground vibration magnitudes.

3. The Vibra Tech model S/N-2222 portable seismograph produced accurate results under identical blasting conditions.

4. Ground vibrations for water-coupled PETN charges were significantly higher than those for air-coupled charges under otherwise identical conditions.

A description of the procedure for the preliminary tests and a listing of the data acquired is given in Appendix B. These procedures incorporated the first three conclusions developed in the test work noted above.

The current study used a Vibra-Tech model S/N-2222 four channel portable seismograph. Since only one seismograph was available, a constant scaled distance of 21.3 ft/lb$^{\frac{1}{2}}$ was maintained for all test blasts. Figure 1 illustrates the geophone position relative to the three blastholes. Geophone placement involved the removal of approximately three inches of weak laminated cap rock, the orientation of the radial component of the geophone toward the blast, and covering the geophone with a 50-pound sandbag. The ground motion was measured in three orthogonal directions and recorded on a magnetic cassette tape. Processing of the magnetic tape yielded a printed waveform of the vertical, radial, and transverse components.

D. DRILLING AND EXPLOSIVES PREPARATION

The selection of a 0.50-inch diameter charge and the associated design dimensions resulted in a practical quanity of rock to be handled from each blast, and it also conformed with charge diameters used in

previous studies of this nature. Atlas Extra Dynamite was selected for this study, and the charges were bottom primed with Dupont electric blasting caps. Explosive properties are outlined in Table A-II. Blastholes were delayed on 25-millisecond intervals, using the initiation sequence illustrated in Figure 1, however, drilling and explosive loading procedures differed between the fully coupled and decoupled test blasts.

1. Fully-Coupled Test. The initial portion of the experimental work for this study required drilling 0.50-inch diameter vertical blastholes, thus allowing direct contact between the 0.50-inch diameter explosive charge and the borehole walls. Air powered equipment capable of drilling 0.50-inch diameter holes was not readily available; therefore, an electric Milwaukee hammer drill powered by a portable generator was used. This type of drill is designed for drilling depths of several feet; however, drill bits in lengths necessary for this study could not be obtained. The only alternative was to manufacture a set of drill steels by welding a two-foot and a four-foot extension onto the two six-inch-long rotary percussion drill bits that were available. This produced a usable drilling system, but by no means a perfect one. Drilling rates for this system were extremely slow because of the drills inherent inability to exhaust the rock cuttings while drilling, and because of the excessive bit wear. frequent removal of the drill steel was necessary so that the rock cuttings could be blown out with compressed air, and the bits resharpened. Once the drilling cycle was completed, blasting caps were lowered into each hole, and the explosive loading procedure began.

The explosive loading procedure for the fully coupled test differed from the other test blasts, in that the explosive was not encased in polyethylene tubing, but rather bulk loaded into the holes. To ensure reliable explosive consistency the charge weight was divided into five sections, and loaded incrementally. After each sectional charge weight was loaded into the hole, the depth to the charge column was measured. Close monitoring of the loading process yielded an explosive consistency comparable to that of the encased charges.

2. Decoupled Tests. Pneumatic drills were used to drill all the boreholes for the decoupled tests. The dynamite was removed from its regular packaging, loaded into 0.50-inch I.D. polyethylene tubing, sealed at each end, and an electric blasting cap inserted at the bottom. Since the encased charge diameter was less than the hole diameter a void space or annulus was formed between the explosive and the rock. The selected coupling medium, water or air, filled this annulus to the top of the charge. A spacer, fashioned from the original wrapping of the explosive was placed directly above the charge to prevent the dry-sand stemming material from falling into the annulus.

E. FRAGMENT SIZING

Immediately after blasting, the oak timbers and sheets of polyethylene were removed. The coarsest fractions of +12, +6-12, and +3-6 inches were hand screened, weighed, and discarded at the test site. The minus 3-inch material was collected in boxes, weighed, removed from the quarry, and later screened into five fractions on a vibratory screen. Each of the eight size fractions, ranging from plus 12-to minus 3/16-inches, were weighed and its percentage of the total rock mass was calculated.

IV. METHODS OF EVALUATING EXPERIMENTAL RESULTS

The basic data resulting from the test blasts included (1) screen size analysis of the fragments by weight, as shown in Table C-I; (3) peak particle velocity measurements in three orthogonal directions for each blast, as shown in Table D-I; and (3) burden-rock contour maps and pictures of each blast before and after firing, Figures E-1 through E-33.

A. FRAGMENTATION

The screen size analysis was evaluated for the purposes of identifying the details of the size distribution and for determining the overall degree of fragmentation for each test blast. A combination of linear least-square and cumulative weight percent curves, histograms, and fragmentation indices were used as correlation techniques. Each of these performed a specific function in describing, illustrating, quantifying, and comparing fragmentation.

1. Evaluation Using Individual Size Fractions. Linear least-square curves of geometric coupling versus weight percent for each individual size fraction are shown in Figures F-1 through F-8. Each of these graphs also illustrate the differences in fractional weight-percents when using air and water as coupling mediums.

2. Evaluation of Overall Fragmentation. Histograms or bar charts, are a common approach for graphically illustrating the size distribution for an individual test blast. A series of histograms were developed using the fraction size versus their corresponding weight percents. Those are paired in Figures 9 through 15, to provide comparison of size distributions between water-and-air-coupled explosives for identical geometric coupling ratios. Figures 14 through 15 are

presented individually, since only one coupling medium was used for each of these test blasts. A 50-percent passing-point is also indicated on all histograms; the position of this point is representative of the overall degree of fragmentation.

The histograms, however, can not mathematically express the size distribution with a single numerical value for comparison purposes. Therefore, the single-term fragmentation index, for expressing the overall fragment-size distribution, that was developed by Smith, (1976), and later used by Brinkmann, (1982), was adopted for this study. The overall fragmentation index, F_c, is a dimensionless value representing the centroidal distance of the composite area of all the size fractions in a histogram. A low F_c value corresponds to a short centroid distance relative to the zero point, and consequently a high degree of overall fragmentation. Table G-I lists the value of F_c for each test, and the positions of the centroids are indicated on the histograms.

3. Evaluation Using Categorized Size Ranges. Selected individual size fractions were grouped according to coarse, medium, and fine material, which correspond to fractional groupings of cumulative +6-in., +3/4-6 in., and cumulative -3/4-in., respectively. Those particular ranges are defined on the basis of realistic sizes of a prototype when using a scaling factor, K, ranging from 10 to 15. The coarse size is considered as being generally oversize, the medium as being a crushable size, and the fine as being the material passing the discharge setting for aprimary crusher typical of the prototype. A graph showing the geometric coupling versus the corresponding cumulative weight percent for each size range is presented in Figure 8,

allowing comparision between coupling media. The respective cumulative weight percentages in each range for individual tests are given in Table G-I.

B. ROCK YIELD, OVERBREAK AND TOE

Quantities of the total rock yield, overbreak- -including back-break and endbreak, and resulting toe, were calculated by planimetering the burden-rock contour maps and are given in Table H-I.

C. GROUND VIBRATION

The particle velocity measured in each of the three orthogonal directions is given in Table D-I. Log-log graphs for the peak particle velocity as a function of geometric coupling were constructed for each coupling medium, and are shown in Figure 16.

V. DISCUSSION OF RESULTS

A. FRAGMENTATION

1. Individual Size Fractions. The screen analysis data presented in Table C-I was used to construct least-square curves for each size fraction by plotting weight-percent versus geometric coupling, Figures F-1 through F-8. Every test blast performed in this study is represented on the graphs, and are grouped according to coupling medium. Although test blasts F-1 and W-47 are plotted on the graphs, they were not used in the least-square calculation for the curves, or as bases for forming conclusions. The reason for the exclusion of blast F-1 is due to the abnormal results, caused by the extensive overbreak, which produced an excessive quantity of plus 12-inch material. Blast W-47 corresponds to test S-32 performed by Smith, (1980), and is presented here for illustrative purposes only. The following discussion emphasizes the important points indicated by the size fraction graphs.

Figure F-1 represents the plus 12-inch size fraction, which was the largest fragment size measured. The water-coupled curve follows a logical trend with better fragmentation resulting from increased geometric coupling; however the air-coupled curve has a slope reverse of that for the water-coupled shots, and the creditability of this slope is questionable even though mathematically determined. An explanation for the trend on the air-coupled tests is not presented here other than noting that previous investigators have indicated that the magnitude of this particular size-fraction frequently is erratic.

Figure F-2 illustrates the screen analysis results for the +6-12-inch fraction. The water-coupled test results appear to be somewhat erratic, in relation to the linear least-squares curve, and possibly the curve should be exponential. The air-coupled results follow a more reasonable linear trend of better fragmentation with increased geometric coupling.

The graph for the largest size-fraction in the medium range, +3-6-inch, presented in Figure F-3, very realistically describes the water-air coupling relationship. Both curves show better fragmentation as the geometric coupling increases, with water coupling producing the best fragmentation results. This trend essentially is also represented by the curves in the next two size fractions of +1½-3, and +3/4-1½-in., Figures F-4 and F-5, respectively.

Figures F-6 and F-7 represent the size-fractions of +3/8-3/4 and +3/16-3/8-in., respectively. Both air and water coupling tend to produce lower percentages of this material with increased geometric coupling, with the water coupling having slightly greater magnitudes.

Figure F-8 represents the screen analysis for the finest size-fraction, +0-3/16-inch. In both situations the percentage of fines decrease with decreasing geometric coupling, and air coupling produces a slightly lesser quantity of fines than water.

2. Coarse Size Fragments Versus Geometric Coupling. The coarse size range is developed by combining the weight percentages of the plus 12-inch, and the +6-12-inch fractions, which produce a cumulative percentage of plus 6-inch material. Selection of these size fractions is based on a scaling factor ranging from 10 to 15.

Consequently, this scaling results in a material size for the prototype that would be relatively larger than the feed opening on a 60-inch primary crusher.

Examination of Figure 8 reveals that an inverse linear relationship exists between the geometric coupling and the percentage of material in the coarse size range. This relationship is valid for air and water coupled tests, with water-coupling resulting in better fragmentation than air.

3. Medium Size Fragments Versus Geometric Coupling. Combining the weight percentages of +3-6, +1½-3, and +3/4-1½-inch material forms a cumulative percentage of +3/4-6-inches, which is defined here as the medium size range. Using a scaling factor between 10 and 15, the medium size range can be defined in the prototype as smaller than the feed opening, but larger than the normal discharge setting for a 60-inch primary crusher.

Figure 8 illustrates that a direct linear relationship exists between the percent of medium size material and the corresponding geometric coupling. Water coupling results in better fragmentation by producing a greater percentage of material in this desirable range than air coupling.

4. Fine Size Fragments Versus Geometric Coupling. The fine size range is a combination of +3/8-3/4, +3/16-3/8, and +0-3/16-inch size fractions, which produce a cumulative weight percent of +0-3/4-inches. These fractions are defined as the material size of the prototype that would pass through the discharge setting of a 60-inch primary crusher without being crushed.

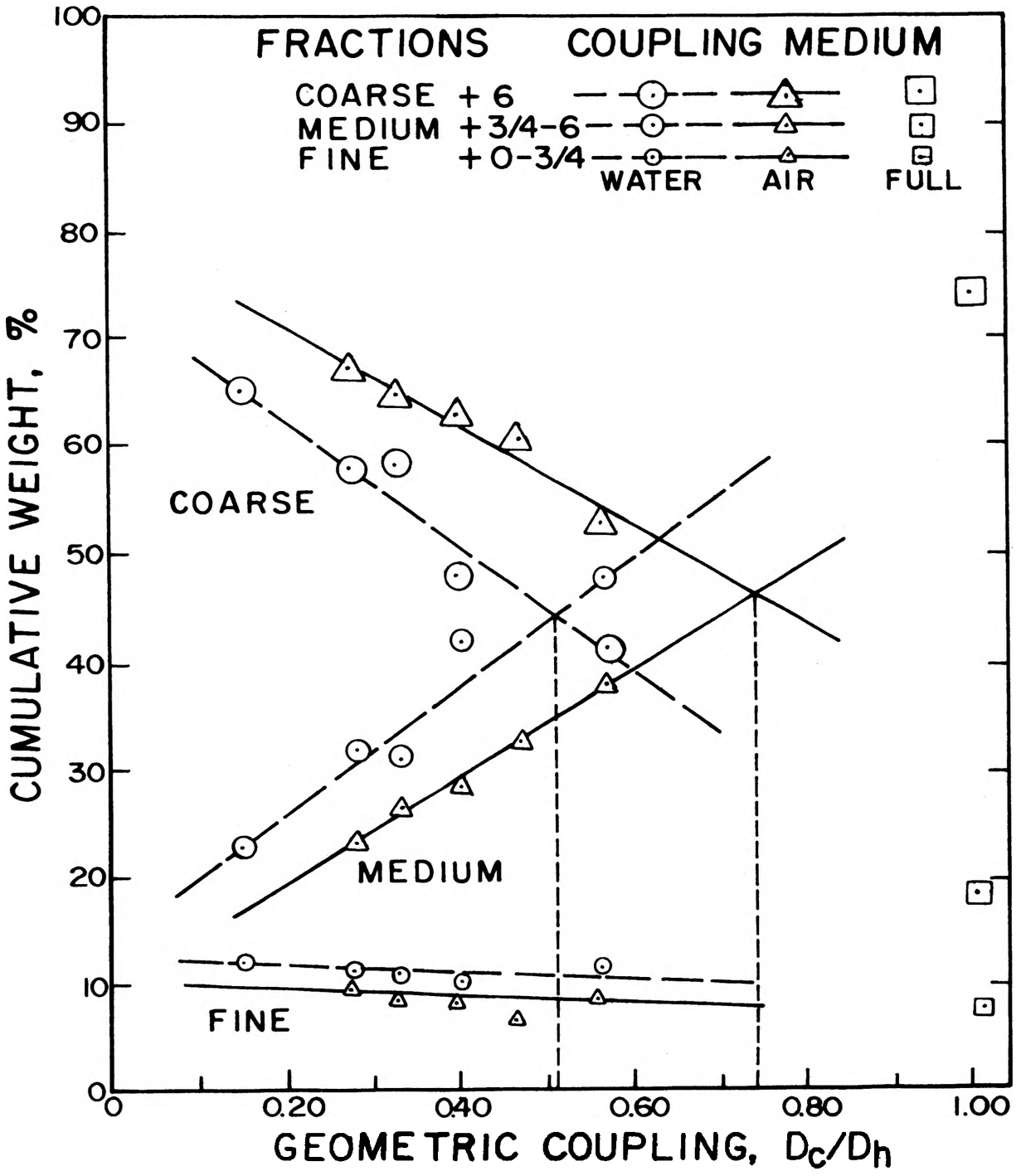

Figure 8. Relationship Between Geometric Coupling and Cumulative Weight Percents in the Coarse, Medium, and Fine Size-Ranges.

Inspection of Figure 8 reveals that water, with low geometric coupling, produces the greatest quantity of fines, while air, with high geometric coupling, produces the least fines.

5. Uniformity. A definition of uniformity relative to fragmentation, can be made on the bases of several parameters. This study, therefore, attempts to define three types of uniformity and relate the fragmentation results from this project to each definition.

First, size range uniformity can be described for all practical purposes as equal percentages of coarse and medium size material, since the fine range in most cases would never reach comparative magnitudes. According to the least-square curves shown on Figure 8, this uniformity is obtained at the intersection of the coarse and medium size range curves for each coupling medium, which correspond to geometric couplings of 0.51 and 0.74, for water and air coupling respectively.

A second type of uniformity can be defined as size-fraction uniformity with a distribution curves superimposed on the histograms presented in Figures 9 through 15. Distribution curves that are right skewed, normal and left skewed are representative of fine, medium, and coarse size material, respectively. The nearer the centroid is to a vertical projection from the peak of a selected distribution curve, the more uniform the product for that situation. In this respect blast W-57 provides the best uniformity in regards to normal and right skewed curves, while blasts A-47 and A-28 reflects the best uniformity for the left skewed curve.

The third type of uniformity requires that the product consist of material in the medium range entirely. In all reality this uniformity

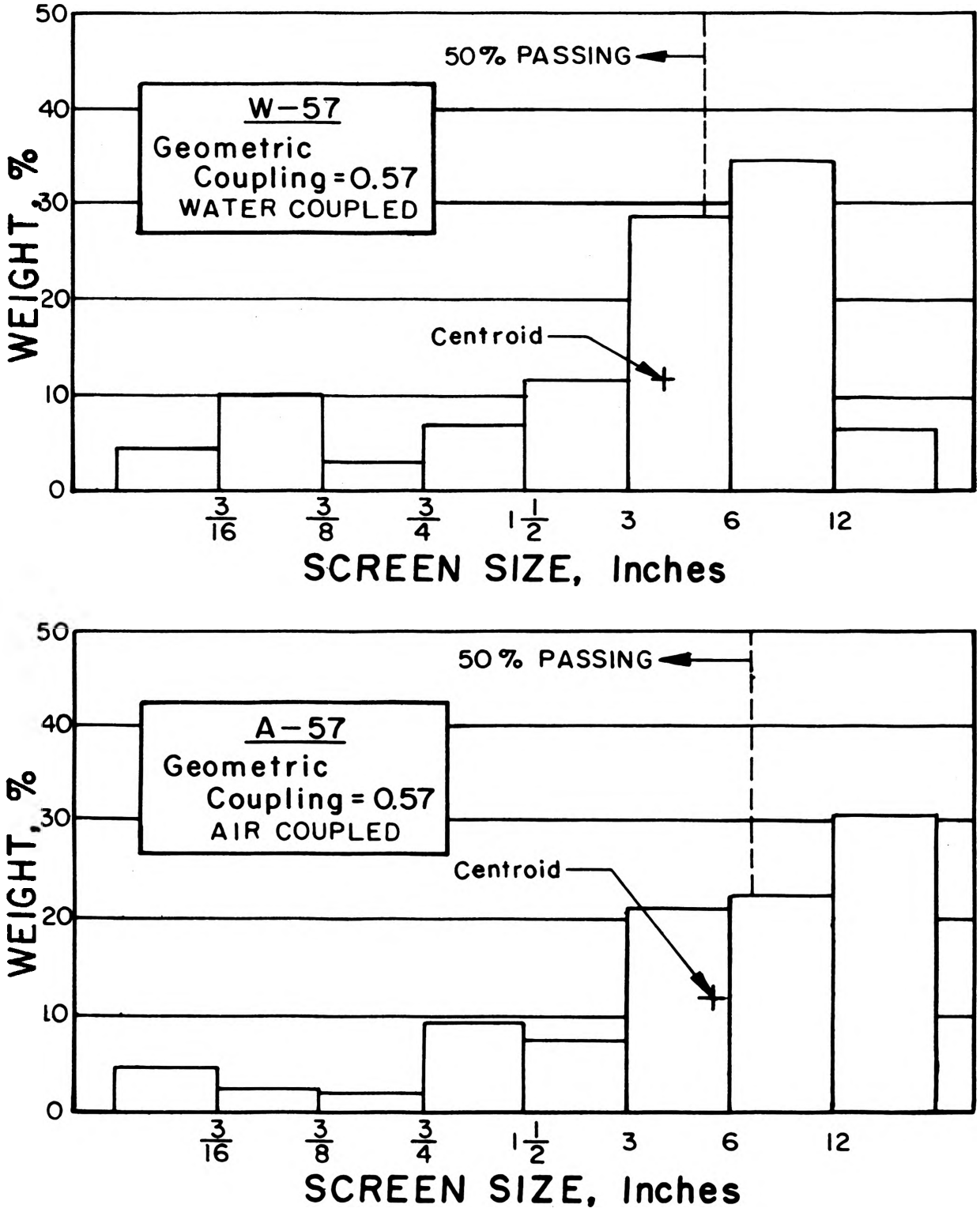

Figure 9. Histograms of Fragment-Size Distribution for Test Blasts with a Geometric Coupling = 0.57.

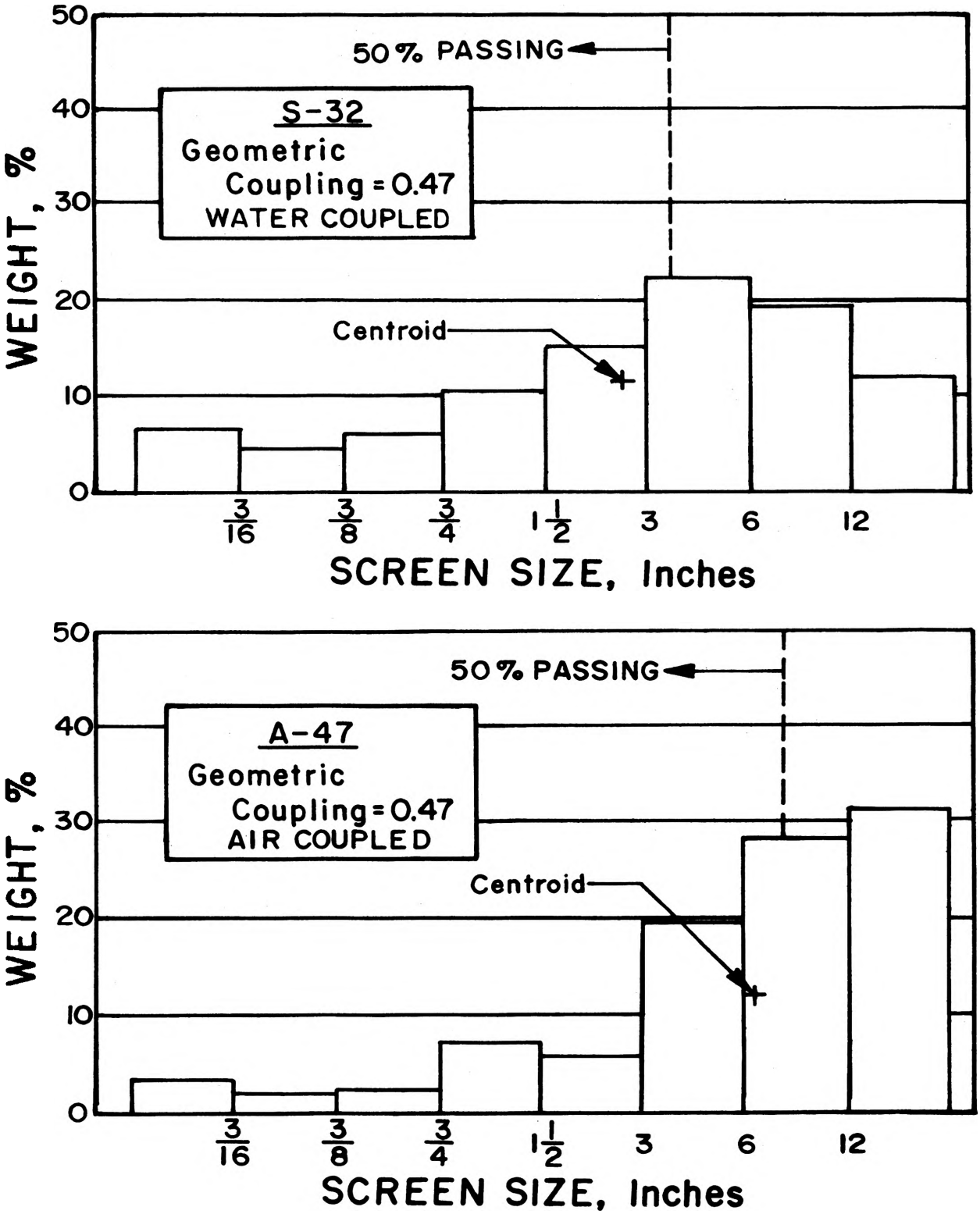

Figure 10. Histograms of Fragment-Size Distribution for Test Blasts with a Geometric Coupling = 0.47. Test S-32 from Smith, (1980).

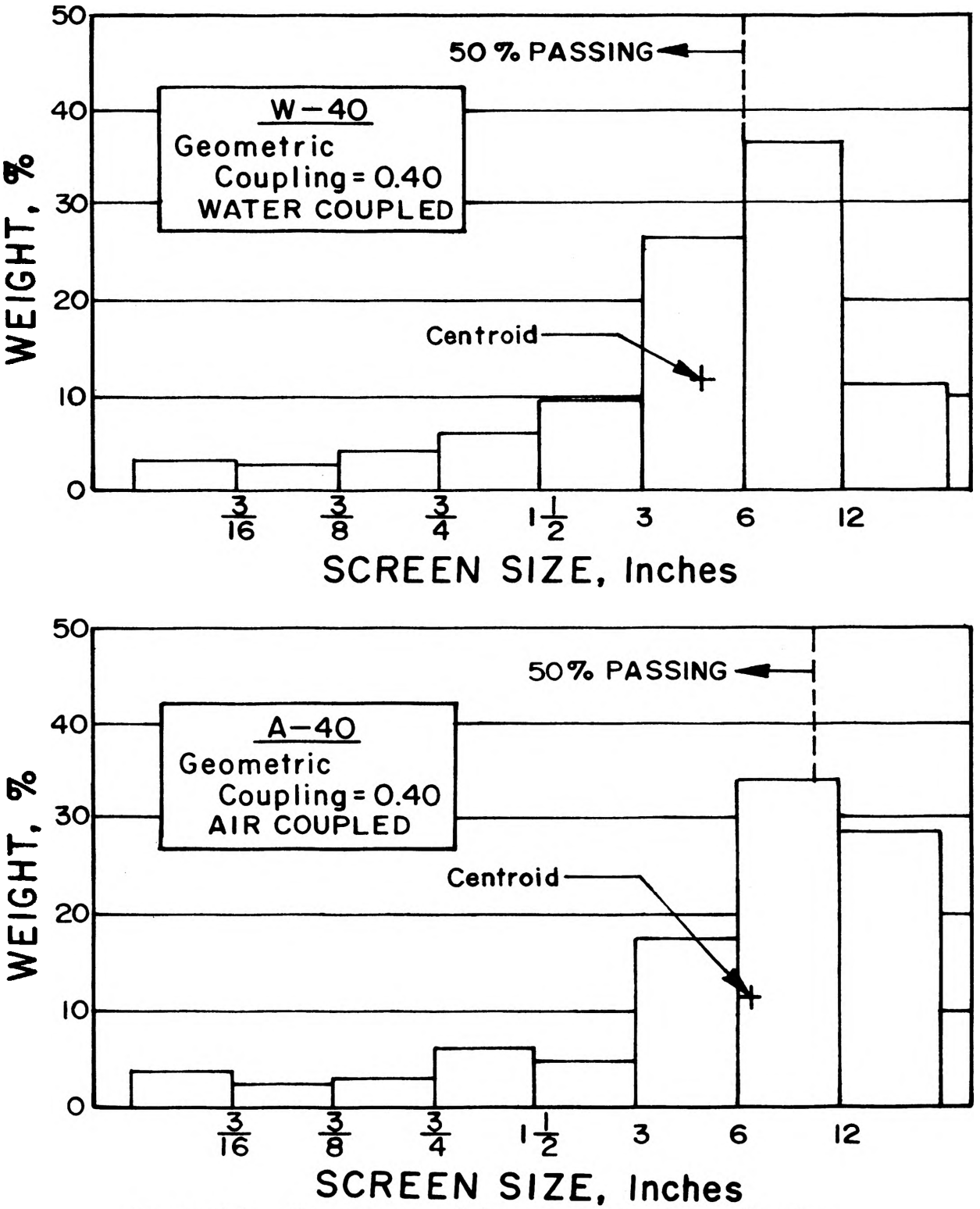

Figure 11. Histograms of Fragment-Size Distribution for Test Blasts with a Geometric Coupling = 0.40.

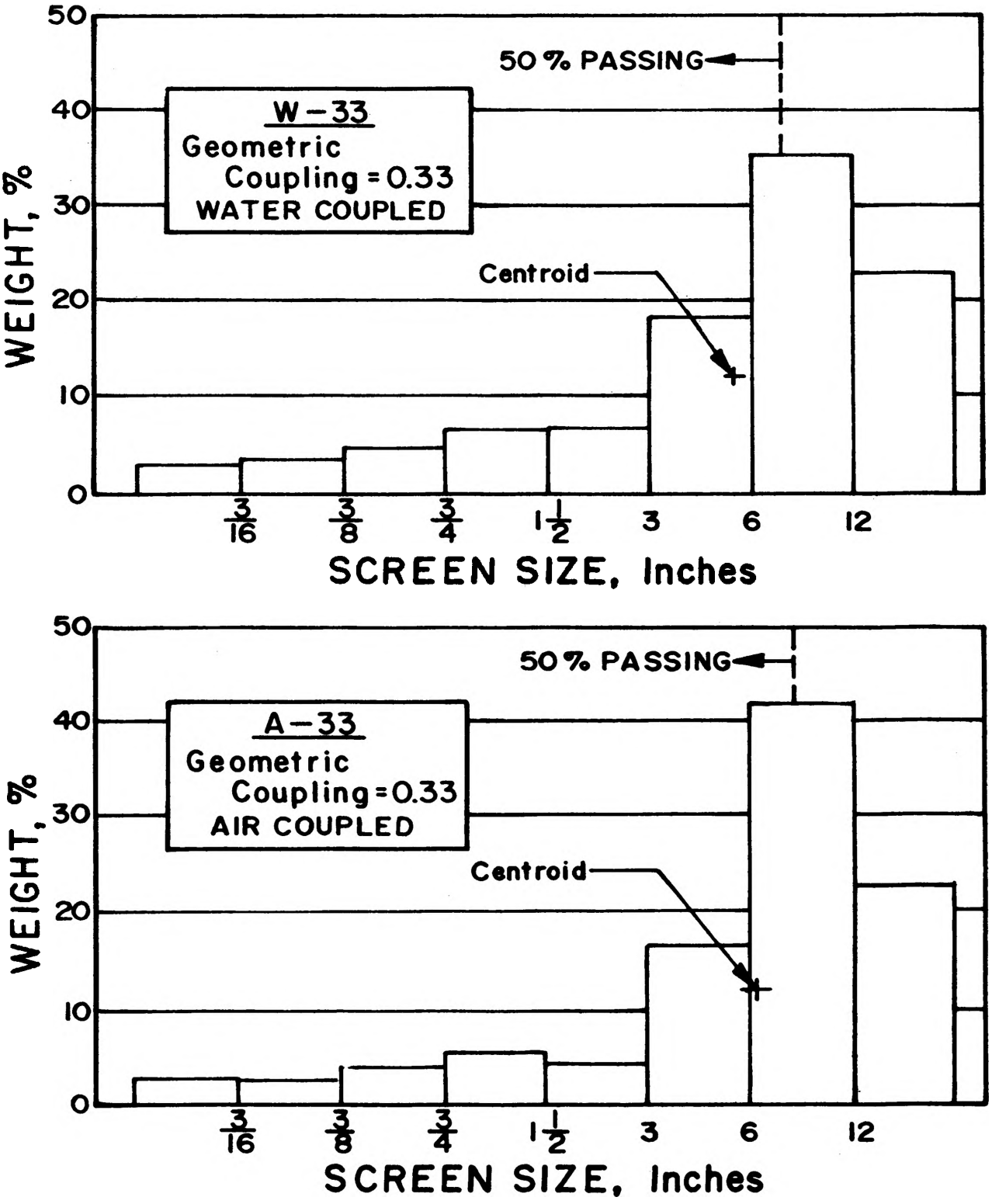

Figure 12. Histograms of Fragment-Size Distribution for Test Blasts with a Geometric Coupling = 0.33.

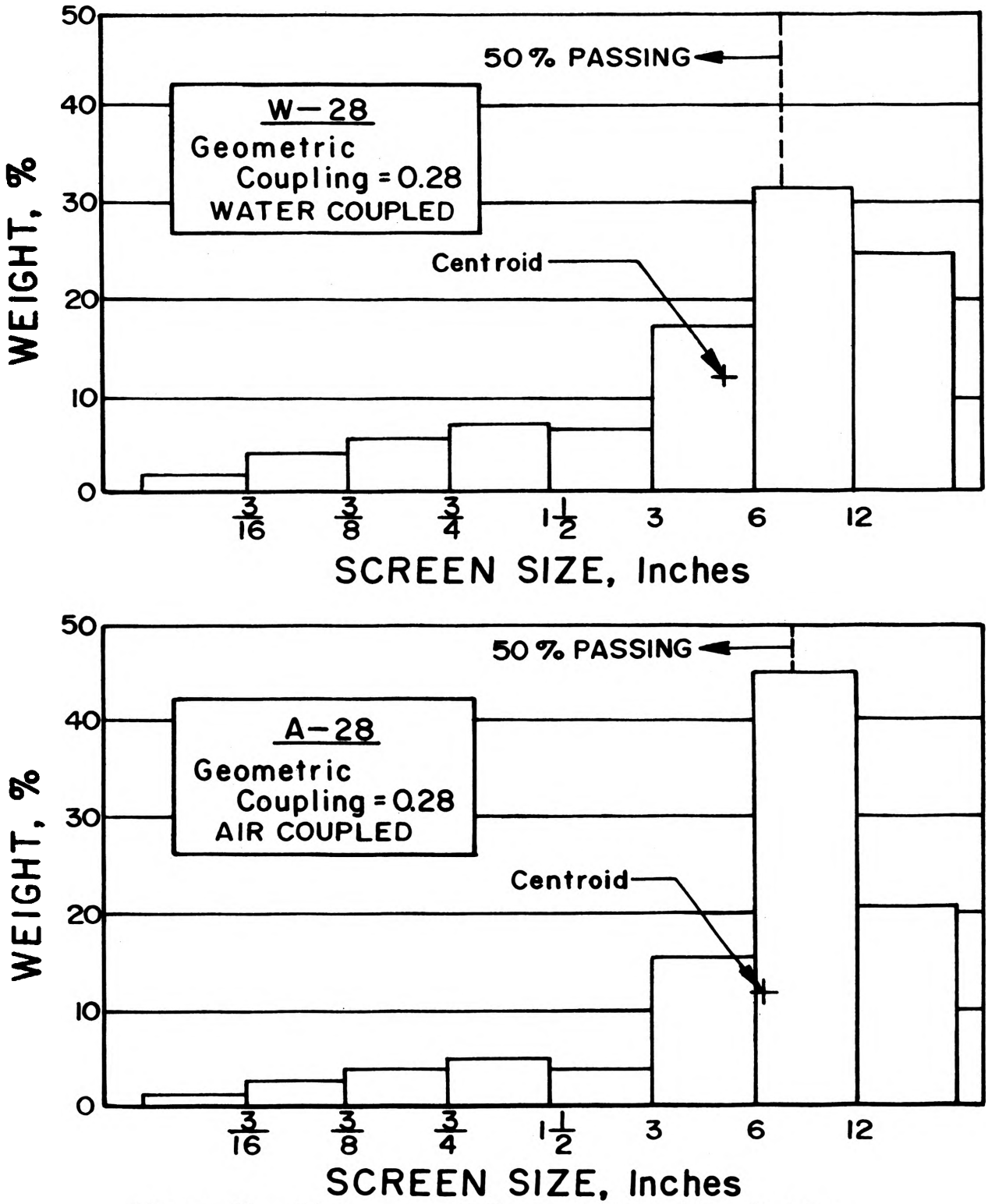

Figure 13. Histograms of Fragment-Size Distribution for Test Blasts with a Geometric Coupling = 0.28.

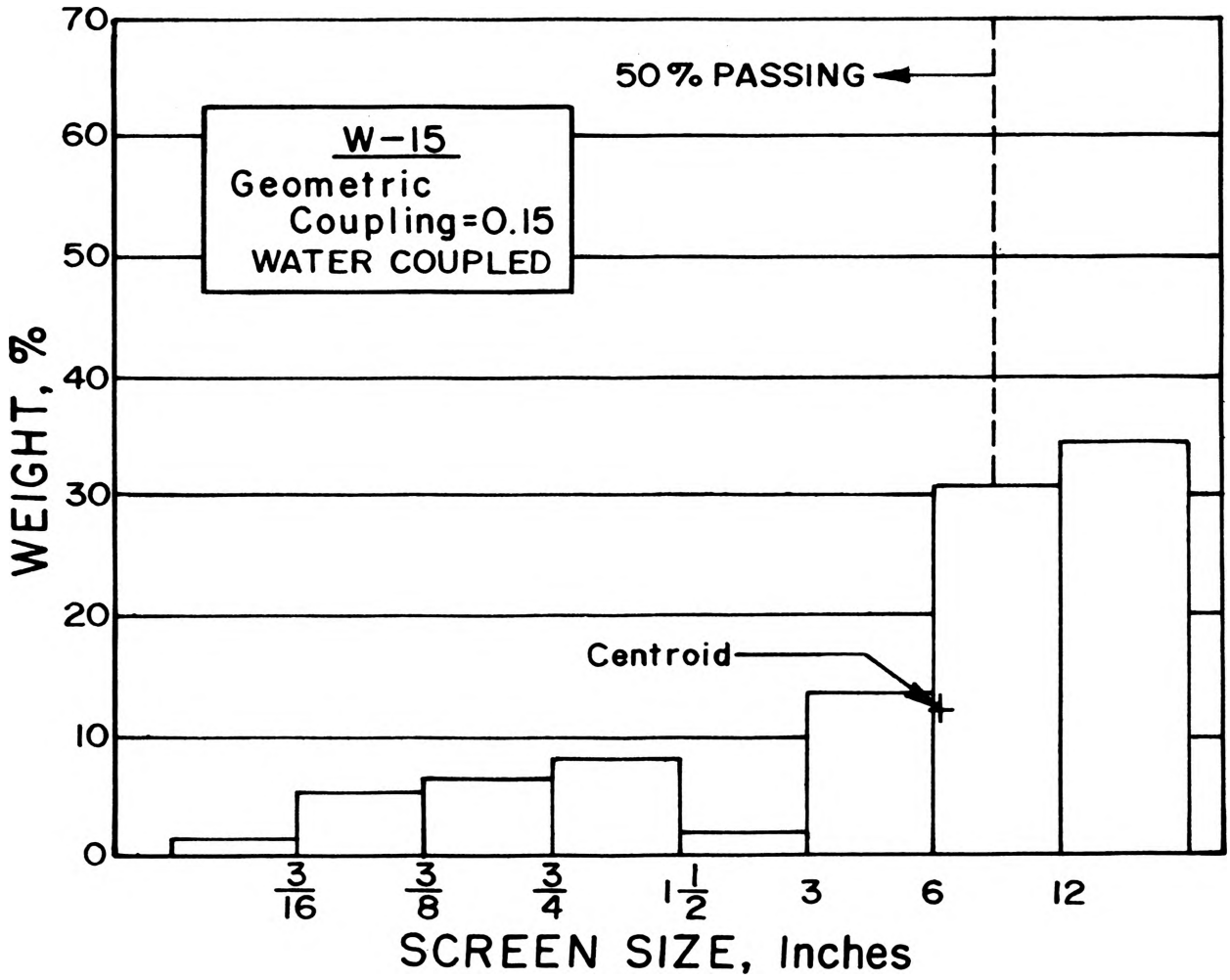

Figure 14. Histograms of Fragment-Size Distribution for Test Blast with a Geometric Coupling = 0.15.

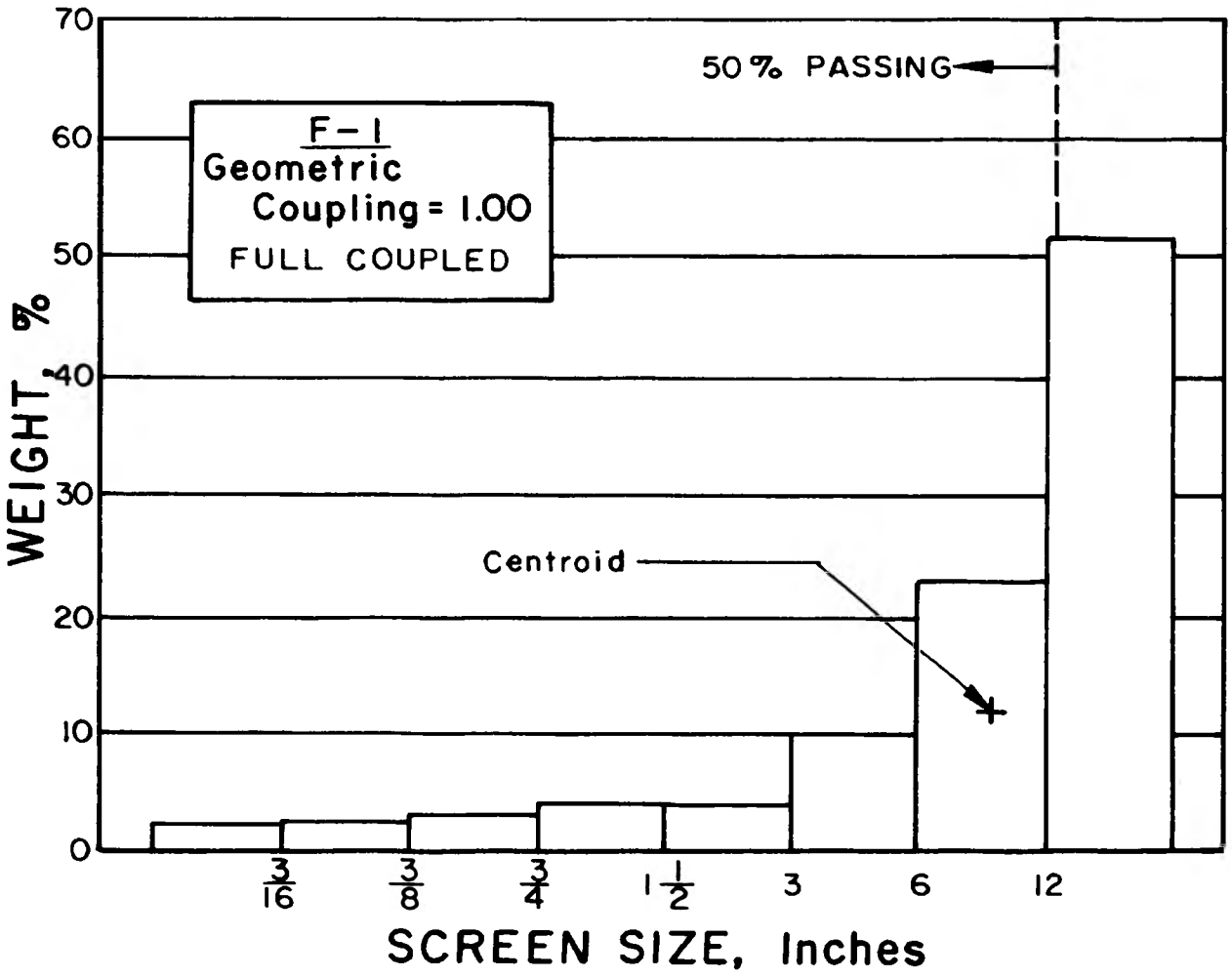

Figure 15. Histograms of Fragment-Size Distribution for Test Blast with a Geometric Coupling = 1.00.

can occur when the medium range is maximized, while the coarse and fine ranges are minimized, without concern with the material quantity in the individual size-fractions for each range. Figure 8 indicates that this type of uniformity could possibly occur at a geometric coupling equal to 1.0; however, for the tests performed the best situation results with blast W-57.

B. GROUND VIBRATION

Peak particle velocity from each test blasts was plotted as a function of geometric coupling on log-log coordinates (Figure 16). This graph illustrates the relative difference in magnitudes of particle velocity between air and water coupling. Inspection of this graph indicates that the effect of geometric coupling with air is much more profound than with water coupling, and that air coupling generally results in higher magnitudes of ground motion.

C. THEORETICAL INTERPRETATION

1. Fragmentation. The decreasing degree of fragmentation experienced with air coupling, when reducing the coupling ratio, entails three considerations: (1) a reduction in detonation pressure which is due to the decreased confinement, (2) a high shock attenuation rate caused by the air layer between the explosive and the rock; and (3) a reduction in the effective borehole pressure is caused by the increasing volume between the charge and the borehole wall, which in turn reduces the tangential stresses in the rock surrounding the borehole.

When a decoupled situation exists, and the annulus is filled with air, the explosive confinement is reduced, thereby decreasing the detonation velocity and pressure. An air annulus between the charge

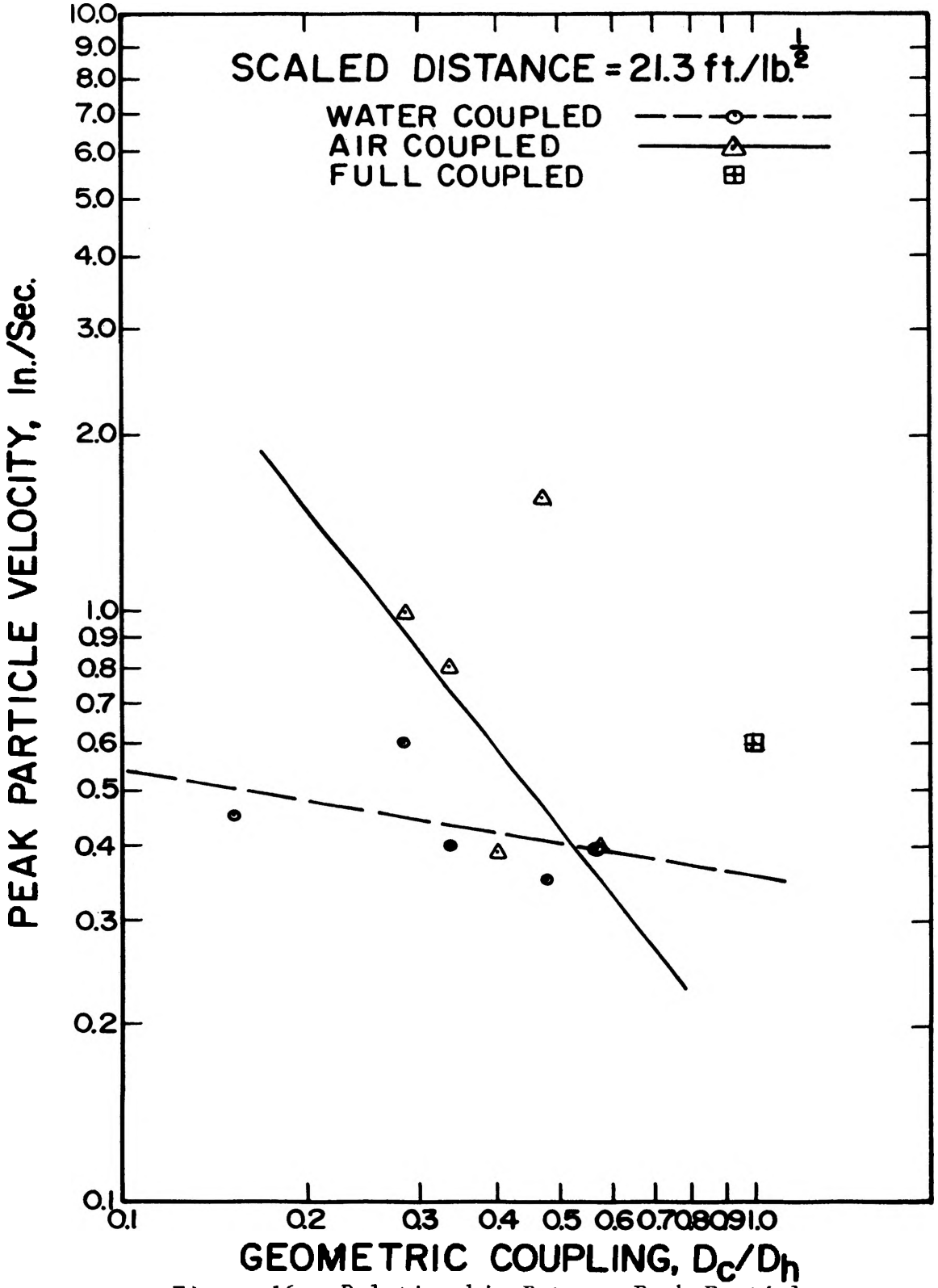

Figure 16. Relationship Between Peak Particle Velocity and Geometric Coupling.

and the rock also causes very high shock attenuation rates as reported by Haas, (1964), which in turn reduces the capability of the detonation front for initiating radial fractures. After passage of the detonation front the explosion gases start expanding to fill the entire borehole. If the borehole volume is larger than that of the original explosive, the effective borehole pressure is less than the explosion pressure. Since the effective borehole pressure is a direct function of the geometric coupling and the explosion pressure, as reported by Ash, (1973), Bergmann, (1974), and Cook, (1958), a reduction in this pressure continues to occur as the geometric coupling is reduced. Using the equations developed by Ash, $P_b = P_e D^2$; Bergmann, $P_b = P_{det} D^{1.90}$; and Cook, $P_b = P_e D^5$, a direct relationship between the calculated effective borehole pressure and the cumulative weight percent of the coarse, medium, and fine size ranges can be demonstrated (Figure 17). The associated tangential stresses within the rock also reduce with increased decoupling, and can be calculated by the standard statics equation for a thick walled cylindrical pressure vessel:

$$S_1 = P_b \frac{b^2 + a^2}{b^2 - a^2}$$

Where:

S_1 = tangential stress, psi;

P_b = calculated effective borehole pressure, psi;

b = outer diameter of cylinder, inches;

a = inner diameter of cylinder, inches.

Table II lists the effective borehole pressure, using Ash's approximation, and associated tangential stresses for each geometric coupling ratio used in this study.

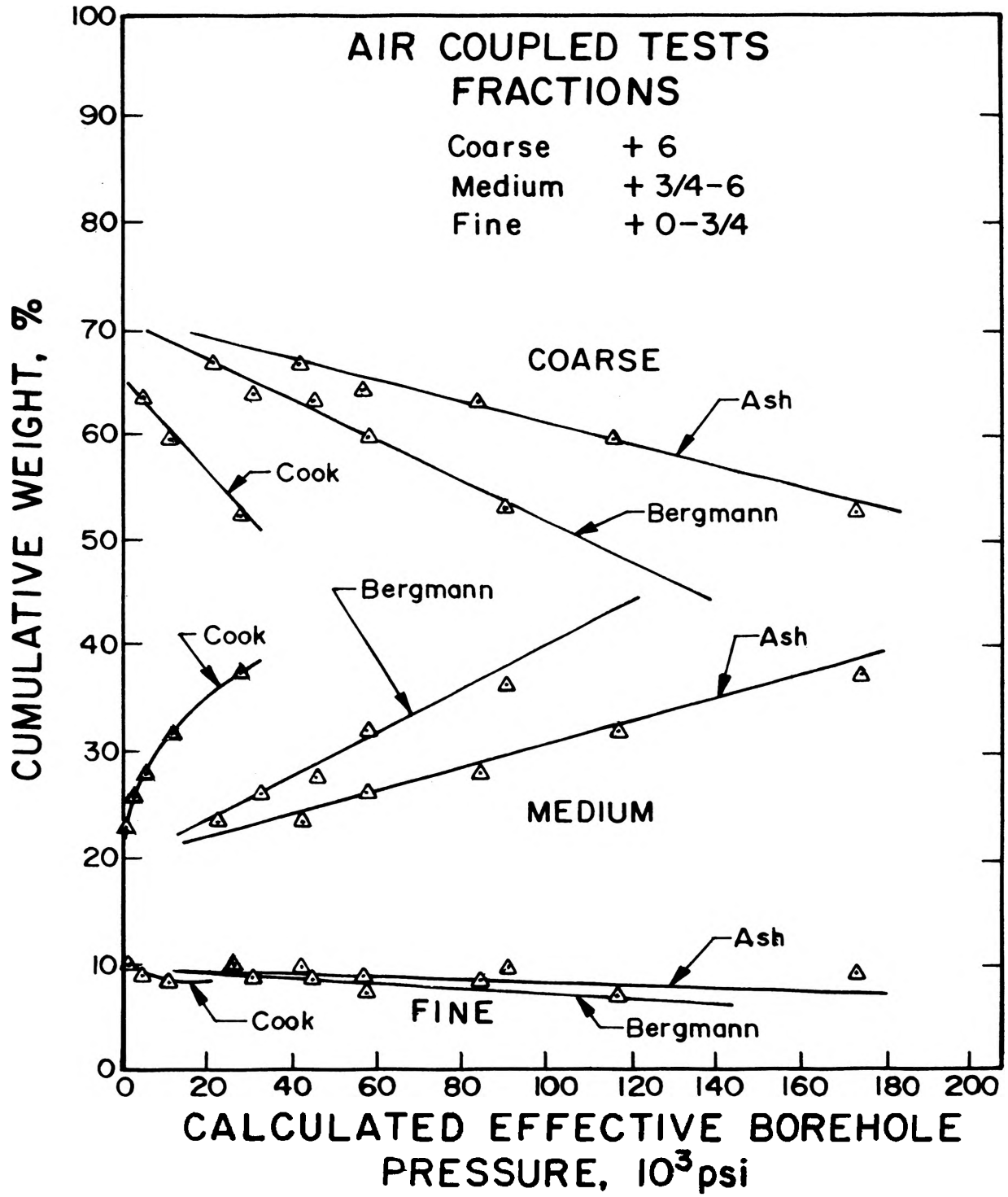

Figure 17. Relationship Between Calculated Effective Borehole Pressure and Coarse, Medium, and Fine Cumulative Weight Percents for Air Coupled Tests.

TABLE II

TANGENTIAL STRESSES FOR

CORRESPONDING GEOMETRIC COUPLING RATIOS

Geometric Coupling	Hole Dia., inches	Effective Borehole Pressure, psi	Tangential Stress, psi
1.00	0.50	536,000	540,000
0.57	0.88	174,000	175,000
0.47	1.06	118,000	119,000
0.40	1.25	86,000	87,000
0.33	1.50	58,000	59,000
0.28	1.75	42,000	43,000
0.15	3.25	12,000	13,000

As indicated in Figure 8, water coupling produces better fragmentation than air coupling. The better fragmentation can be explained on the basis of increased confinement and the low shock attenuation rate associated with water. Increasing the confinement allows a higher detonation pressure to develop, and the actual coupling of water, as reported by Haas, (1964), permits more of the shock energy to be transmitted into the rock mass. The decrease in the degree of fragmentation with decreasing geometric coupling ratios may be caused by a loss of explosive energy, due to the phase change from water to steam, causing a consequent drop in the explosion temperatures, and a reduction in the borehole pressure. Since the borehole pressure drops at a greater rate than the rate of increase in the hole diameter, tangential stresses are reduced as the geometric coupling decreases.

2. Ground Vibrations. The peak particle velocity magnitudes are inversely related to fragmentation results. Air coupling, therefore, generally produces more ground motion than water coupling. This can be explained on the basis of a higher proportion of the explosive energy directed toward rock fragmentation instead of ground vibrations.

D. ROCK YIELD, OVERBREAK AND TOE

The quantities of total rock yield, overbreak, and toe that were found by planimetering the burden-rock contour maps, shown in Figures E-1 through E-33, are presented in Table H-I. There were no significant trends of overbreak or toe associated with the amount of decoupling or the coupling medium, other than the excessive endbreak, backbreak, and toe resulting from the fully-coupled test blast.

VI. CONCLUSIONS

1. Explosive decoupling does have the potential for controlling fragmentation, with an appreciable influence on the quantities of material in the medium and coarse size ranges.

2. The degree of rock fragmentation is directly affected by the amount of decoupling, and the material surrounding the explosive charge.

3. Water coupling results in a higher degree of fragmentation than air-coupling, producing greater quantities of medium size material and lower quantities of coarse material; the quantity of fines decrease slightly as the geometric coupling increases, with water coupling producing more fines than air coupling.

4. The fragmentation results for this investigation correspond to the strain wave magnitudes measured for decoupled blasts on full-scale operations.

5. Ground vibration magnitudes for water-coupled blasts are generally lower than those of air-coupled blasts, and are inversely related to the degree of fragmentation.

VII. RECOMMENDATIONS FOR FURTHER INVESTIGATION

1. A similar series of tests should be conducted using geometric coupling ratios ranging from 0.60 to 1.0.
2. Further investigations could be performed to examine the fragmentation resulting when an explosive charge is decoupled within the column, commonly referred to as the air gap method, and compared to the results of this investigation by using equivalent values of void space volume-to-explosive-volume ratios.
3. A repetition of these tests with identical geometric coupling ratios, altering the charge diameter in the geometric coupling ratio, while maintaining a constant borehole diameter.
4. A set of experiments measuring the actual borehole pressure during blasting, when using various geometric coupling ratios, and relating this measured pressure to the fragmentation results and the calculated effective borehole pressures used in this investigation.

REFERENCES

Ash, R.L., "The Influence of Geological Discontinuities on Rock Blasting." Unpublished PhD Dissertation, University of Minnesota, Minneapolis, 1973.

Attewell, P.B., and Farmer, I.W., "Ground Vibrations from Blasting: Their Generation, Form and Detection." The Quarry Manager Journal, May 1964, pp. 191-198.

Bergmann, O.R., Riggle, J.W., Wu, F.C., "Model Rock Blasting-Effect of Explosives Properties and Other Variables on Blasting Results." Int. J. Rock. Mech. Min. Sci., Vol. 10, (1973), 585-612.

Bhandari, S., "Burden and Spacing Relationships in the Design of Blasting Patterns." Proc. 16th Symp., Rock Mech., Univ. of Minn., 1975.

Bhandari. S., Vutukiri, U.S., "Rock Fragmentation with Longitudinal Explosive Charges." Proc. 3rd Cong. Int. Soc. Rock Mech., Denver, Vol. 2, (1974), 1337-42.

Brinkmann, J.R., "The Influence of Explosive Primer Location on Fragmentation and Ground Vibrations for Bench Blasts in Dolomitic Rock." Unpublished M.S. Thesis, Univ. Of MO-Rolla, 1982.

Casquino, W.T., "The Development of Conical Stress Forms by Explosive Charges." Unpublished M.S. Thesis, Univ. of MO-Rolla, 1965.

Cook, Melvin A., "The Science of High Explosives." New York: Reinold Publishing Company, 1958.

Da Gama, C.D., "Similitude Conditions in Models for Studies of Bench Blasting." Proc. 1st Cong. Int. Soc. Rock. Mech., Belgrade, Vol. 3, (1970).

Da Gama, C.D., "The Size of the Largest Fragment in Rock Blasting." Proc. 3rd Cong. Int. Soc. Rock Mech., Denver, Vol. 2, (1974).

Deatherage, J.H., "The Development of the Sonic Pulse Technique and Its Comparison with the Conventional Static Method for Determining the Elastic Moduli of Rock." Unpublished M.S. Thesis, Univ. of MO-Rolla, (1964).

Dick, R.A., Fletcher, L.R., D'Andrea, D.V., "A Study of Fragmentation From Bench Blasting in Limestone at a Reduced Scale." R.I. 7704 U.S. Bureau of Mines, (1973).

DuPont, E.I., De Nemours and Co., Blasters Handbook. 16th Edition, Wilmington, Delaware, (1977).

Fogelson, D.E., D'Andrea, D.V., Fischer, R.L., "Effects of Decoupling and Type of Stemming on Explosion-Generated Pulses in Mortar." R.I. 6679 U.S. Bureau of Mines, (1965).

Haas, C.J., "Coupling Between Uncontinued Cylindrical Explosive Charges and Rock." Int. J. Rock Mech. Min. Sci., Vol. 22, (1964), 13-24.

Hagan, T.N., Just, G.R., "Rock Breakage by Explosives-Theory, Practice and Optimization." Proc. 3rd Cong. Int. Soc. Rock. Mech., Denver, Vol. 2, (1974).

Hagan, T.N., "The Control of Fines Through Improved Blast Design." Proc. Aust. Inst. Min. Metall., Vol. 271, (Sept. 1979), 9-20.

Johansson, C.H., Persson, P.A., "Detonics of High Explosives." Academic Press Inc., London, (1970).

Johansson, C.H., Persson, P.A., "Fragmentation Systems," Proc. 3rd Cong. Int. Soc. Rock Mech., Denver, Vol. 2, (1974).

Keller, R.L., "Design of Blasthole Initiation Delay Intervals and Apex Angle for Optimum V-Cut Cratering." Unpublished M.S. Thesis, Univ. of MO-Rolla, (1982).

Kolsky, H., "Stress Waves in Solids." Dover Publications, New York, (1963).

Langefors, V., Kihlstrom, B., "The Modern Technique of Rock Blasting." John Wiley and Sons, New York, (1967).

Melinkov, N.V., "Influence of Explosive Charge Design on Results of Blasting." Int. Symp. on Min. Res., Vol. 1, (1962).

Melinkov, N.V., "Method of Enhanced Rock Breakage by Blasting." Sov. Min. Sci., Vol. 15, (Nov-Dec., 1979), 565-572.

Nicholls, H.R., "Coupling Explosive Energy to Rock." Geophysics, Vol. 27, (June, 1962).

Persson, P.A., Ladergaard-Pederson, A., Kihlstrom, B., "The Influence of Borehole Diameter on Rock Blasting Capacity of an Extended Charge." Int. J. Rock Mech. Min. Sci., Vol. 6, (May, 1969).

Quan, K.C., "The Characteristics of Radial Strain Propogation Induced By Explosive Impact in Jefferson City Dolomite." Unpublished M.S. Thesis, Univ. of MO-Rolla, (1964).

Smith, N.S, "Burden-Rock Stiffness and Its Effect on Fragmentation in Bench Blasting." Unpublished PhD Dissertation, Univ. of MO-Rolla, (1976).

Smith, N.S., "An Investigation of the Effects of Blasthole Confinement on the Generation of Ground Vibrations in Bench Blasting." Unpublished Report, SMI Grant Sect. 301, (1980).

Taqieddin, S.A., "The Role of Borehole Pressure Containment on Surface Ground Vibration Levels at Close Scaled Distances." Unpublished PhD Dissertation, Univ. of MO-Rolla, (1982).

Ucar, R., "Decoupled Explosive Charge Effects on Blasting Performance." Unpublished M.S. Thesis, Univ. of MO-Rolla, (1975).

Worsey, P., "Geotechnical Factors Affecting the Application of Pre-Split Blasting to Rock Slopes." Unpublished PhD Thesis, Univ. of New Castle, England, (1981).

VITA

Timothy Wayne Warden was born on January 26, 1959 in Beckley, West Virginia. He received his elementary and secondary education in Beckley, West Virginia, and his college education from Beckley College in Beckley, West Virginia, and West Virginia Institute of Technology in Montgomery, West Virginia. In May of 1981 he received a Bachelor of Science Degree in Mining Engineering Technology from West Virginia Institute of Technology.

From June 1, 1981 until January 1, 1982, he held the postion of Utility Supervisor for Black River Lime Company, in Butler, Kentucky, an underground limestone producer, and lime manufacturer. He then entered graduate school at the University of Missouri-Rolla, and expects to receive a Master of Science Degree in Mining Engineering in May, 1983. While attending graduate school he held a Mining Engineering Teaching Assistantship, a Chancellor's Fellowship, and was awarded the AIME Henry De-Witt Smith graduate scholarship.

APPENDIX A

PROPERTIES OF DOLOMITIC ROCK MEDIUM AND EXPLOSIVE USED IN TEST BLASTS

TABLE A-I

PROPERTIES OF JEFFERSON CITY FORMATION DOLOMITIC ROCK

(Deatherage (1966) and Casquino (1965)

PHYSICAL PROPERTIES:

90% Dolomite

10% Calcite

Tan to gray color

Massive bedding

Texture - crystalline; irregular and non-uniform shape and size of crystal; matrix is mainly dolomite

Specific Gravity 2.677

ELASTIC PROPERTIES:

Compressive Strength (dry)	9,000 psi
Tensile strength (dry)	200 psi
Shear Strength (dry)	7,500 psi
Poisson's Ratio (dry)	0.27
Young's Modulus (static)	2.18×10^6 psi
(dynamic)	2.26×10^6 psi
Longitudinal velocity (dry)	14,800 fps
Shear Velocity	8,100 fps

TABLE A-II

CHARACTERISTIC OF EXPLOSIVE

USED IN TEST BLASTS

(Ash, 1973)

Type: Ammonia Dynamite, 60 Percent Strength

Cartridge Count: 112 per 50-lb case, 1¼ x 8 inches

Ideal Performance Specifications:			
Specific Gravity:		1.29	
Heat of Formation:	-1008		kcal/kg
Heat of Explosion:	- 702		kcal/kg
Detonation Temperature:	2930		Degree K
Detonation Pressure:	83.2		kbar
Detonation Velocity:	17,700		fps
Measured Field Performance Specifications:			
Specific Gravity		1.12	
Detonation Velocity:	12,800		fps @ 1¼" dia.
	11,300		fps @ 7/8" dia.
	8,400		fps @ ½" dia.
Estimated Field Performance Pressures:			
Maximum Detonation Pressure:	74		kbar
(adjusted to 1.12 Specific gravity)			
Borehole Pressure:	37		kbar
(0.5 Max. Det. Pressure)			
Detonation Pressure at			
Velocity 8,400 fps			
Cook's Approximation	18.3		kbar
Brown's Approximation	17.4		kbar
Dick's Approximation	17.6		kbar

APPENDIX B

PROCEDURES AND RESULTS FOR PRELIMINARY TESTS

APPENDIX B

PROCEDURE FOR PRELIMINARY TESTS

A total of fifteen test blasts were performed in three separate sets of experiments for the purpose of evaluating the accuracy of the Vibra-Tech Model S/N-2222 protable seismograph, determining the relative differences between water-and-air-coupled explosive charges on peak particle velocity magnitudes, and finding the most suitable sandbag weight to couple the geophone to the ground. The resulting peak particle velocity magnitudes for each blast were taken from the meter display on the seismograph. Geophone position and charge weight remained the same for all tests, providing a constant scaled distance of 21.5 $ft/lb^{\frac{1}{2}}$. Parameters that remained constant throughout these preliminary tests were: explosive charge weight which was 200 gr/ft. of primacord in three foot lengths, geophone distance of six feet, the hole length of forty inches, and hole diameter of 1-1/16-inches. A single borehole was drilled for each set of experiments and used throughout that particular series for blasting.

The repeatability of the portable seismograph was determined by measuring the peak particle velocity for five identical blasts and comparing the results (Table B-I). The relative difference of peak particle velocity magnitudes, between air-and-water-coupled PETN charges was evaluated with four blasts (Table B-II). A series of six blasts were performed to determine the sandbag weight necessary on the geophone to provide adequate coupling (Table B-III).

The entire series of preliminary tests were performed for the purpose of standardizing ground vibration measurement procedures for subsequent experimentation.

TABLE B-I

SEISMOGRAPH ACCURACY TEST RESULTS*

(TEST SITE A)

Blast No.	Peak Particle Velocity, in/sec.
1	0.62
2	0.65
3	0.60
4	0.65
5	0.64

*Water was used as the coupling medium for all blasts.

TABLE B-II

PRELIMINARY COUPLING MEDIUM TEST BLAST RESULTS

(TEST SITE B)

Blast No.	Coupling Medium	Peak Particle Velocity, in/sec.
1	Water	0.85
2	Water	0.82
3	Air	0.14
4	Air	0.19

TABLE B-III

GEOPHONE COUPLING PRELIMINARY TEST BLAST RESULTS*

(TEST SITE C)

Blast No.	Geophone Weight lbs	Peak Particle Velocity, in/sec.
1	0	1.50
2	0	1.00
3	50	0.85
4	50	0.89
5	100	0.69
6	100	0.80

*Water was used as the coupling medium for all blasts.

APPENDIX C

SCREEN ANALYSES OF TEST-BLAST FRAGMENTATION

TABLE C-I

SCREEN ANALYSES OF TEST-BLAST FRAGMENTATION

Blast No.	Specification	Fragment Size Fraction (inches) -3/16	+3/16-3/8	+3/8-3/4	+3/4-1½	1½-3	+3-6	+6-12	+12
F-1	Weight (lb)	144	166	198	264	253	650	1481	3338
	Weight %	2.2	2.5	3.0	4.1	3.9	10.0	22.8	51.4
A-57	Weight (lb)	198	114	93	379	316	902	940	1272
	Weight %	4.7	2.7	2.2	9.0	7.5	21.4	22.3	30.2
A-47	Weight (lb)	142	77	94	297	240	807	1180	1304
	Weight %	3.4	1.8	2.3	7.2	5.8	19.5	28.5	31.5
A-40	Weight (lb)	140	92	105	230	170	669	1288	1084
	Weight %	3.7	2.4	2.8	6.1	4.5	17.7	34.1	28.7
A-33	Weight (lb)	96	86	143	196	154	603	1506	786
	Weight %	2.7	2.4	4.0	5.5	4.3	16.9	42.2	22.0
A-28	Weight (Lb	46	96	185	126	132	515	1517	687
	Weight %	1.4	2.9	5.6	3.8	4.0	15.6	45.9	20.8

TABLE C-I (continued)

SCREEN ANALYSIS OF TEST BLAST FRAGMENTATION

Blast No.	Specification	Fragment Size Fraction (inches)							
		-3/16	+3/16-3/8	+3/8-3/4	+3/4-1½	+1½-3	+3-6	+6-12	+12
W-57	Weight (lb)	186	165	128	285	487	1181	1424	273
	Weight %	4.5	4.0	3.1	6.9	11.8	28.6	34.5	6.6
W-40	Weight (lb)	104	99	144	206	303	885	1211	376
	Weight %	3.1	3.0	4.3	6.2	9.1	26.6	36.4	11.3
W-33	Weight (lb)	125	152	206	295	287	806	1581	1026
	Weight %	2.8	3.4	4.6	6.6	6.4	18.0	35.3	22.9
W-28	Weight (lb)	68	161	229	286	266	705	1305	1007
	Weight %	1.7	4.0	5.7	7.1	6.6	17.5	32.4	25.0
W-15	Weight (lb)	46	203	253	336	70	551	1276	1409
	Weight %	1.1	4.9	6.1	8.1	1.7	13.3	30.8	34.0

APPENDIX D

LONGITUDINAL, VERTICAL, AND TRANSVERSE PEAK PARTICLE VELOCITIES FOR TEST BLASTS

TABLE D-I

LONGITUDINAL, VERTICAL, AND TRANSVERSE

PEAK PARTICLE VELOCITIES FOR TEST BLASTS*

Blast No.	Geometric Coupling	Coupling Medium	Peak Particle Velocity, in./sec. Longi-udinal	Vertical	Trans-Verse
F-1	1.00	Full	0.60	0.60	0.50
A-57	0.57	Air	0.20	0.40	0.30
A-47	0.47	Air	1.60	1.60	1.40
A-40	0.40	Air	0.40	0.40	0.40
A-33	0.33	Air	0.60	0.80	0.60
A-28	0.28	Air	0.80	0.80	1.00
W-57	0.57	Water	0.30	0.30	0.40
**W-47	0.47	Water	0.15	0.35	0.30
W-40	0.40	Water	NR	NR	NR
W-33	0.33	Water	0.10	0.40	0.10
W-28	0.28	Water	0.50	0.60	0.60
W-15	0.15	Water	0.20	0.45	0.20

NR - No reading due to equipment failure

*Scaled distance = 21.3 ft/lb$^{\frac{1}{2}}$ for all blasts.

**Smith shot S-32, (1980).

APPENDIX E

BURDEN-ROCK CONTOUR MAPS, VERTICAL SECTIONS, AND PHOTOGRAPHS FOR TEST BLASTS

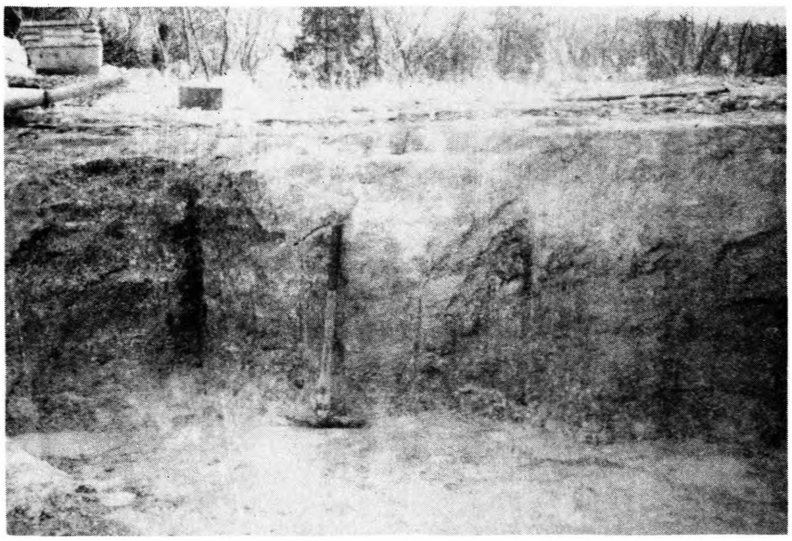

Figure E-1. Bench for Test F-1 Before Blasting.

Figure E-2. Bench for Test F-1 After Blasting.

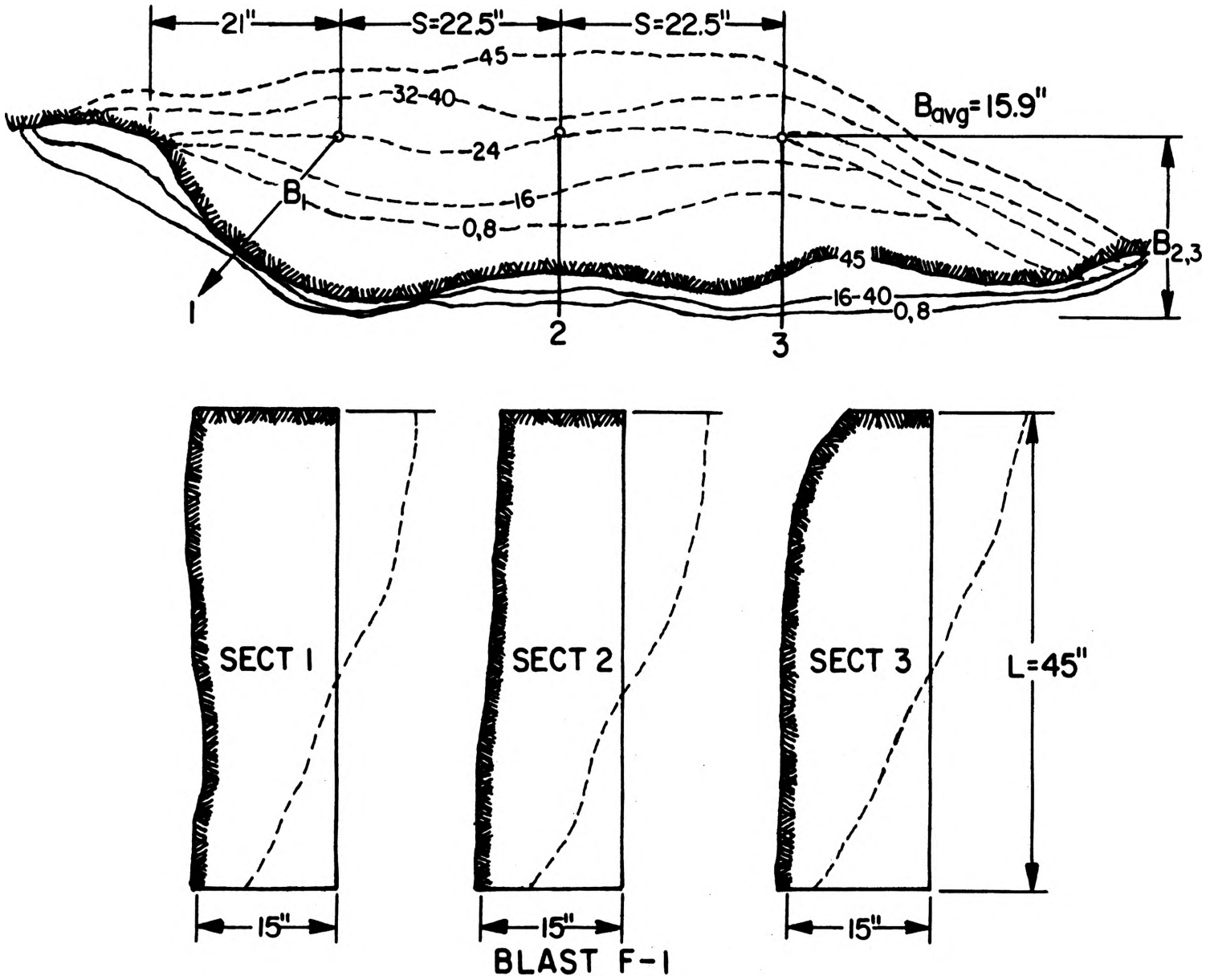

Figure E-3. Burden-Rock Contour Map and Vertical Sections for Test F-1.

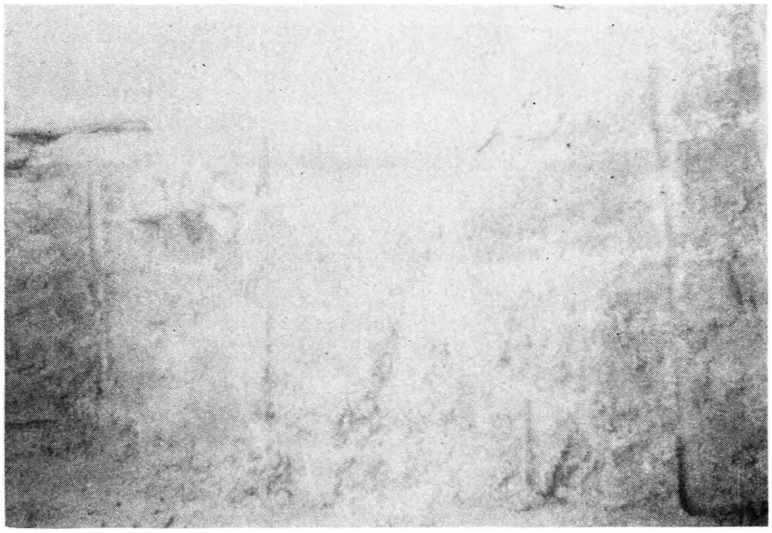

Figure E-4. Bench for Test W-57 Before Blasting.

Figure E-5. Bench for Test W-57 After Blasting.

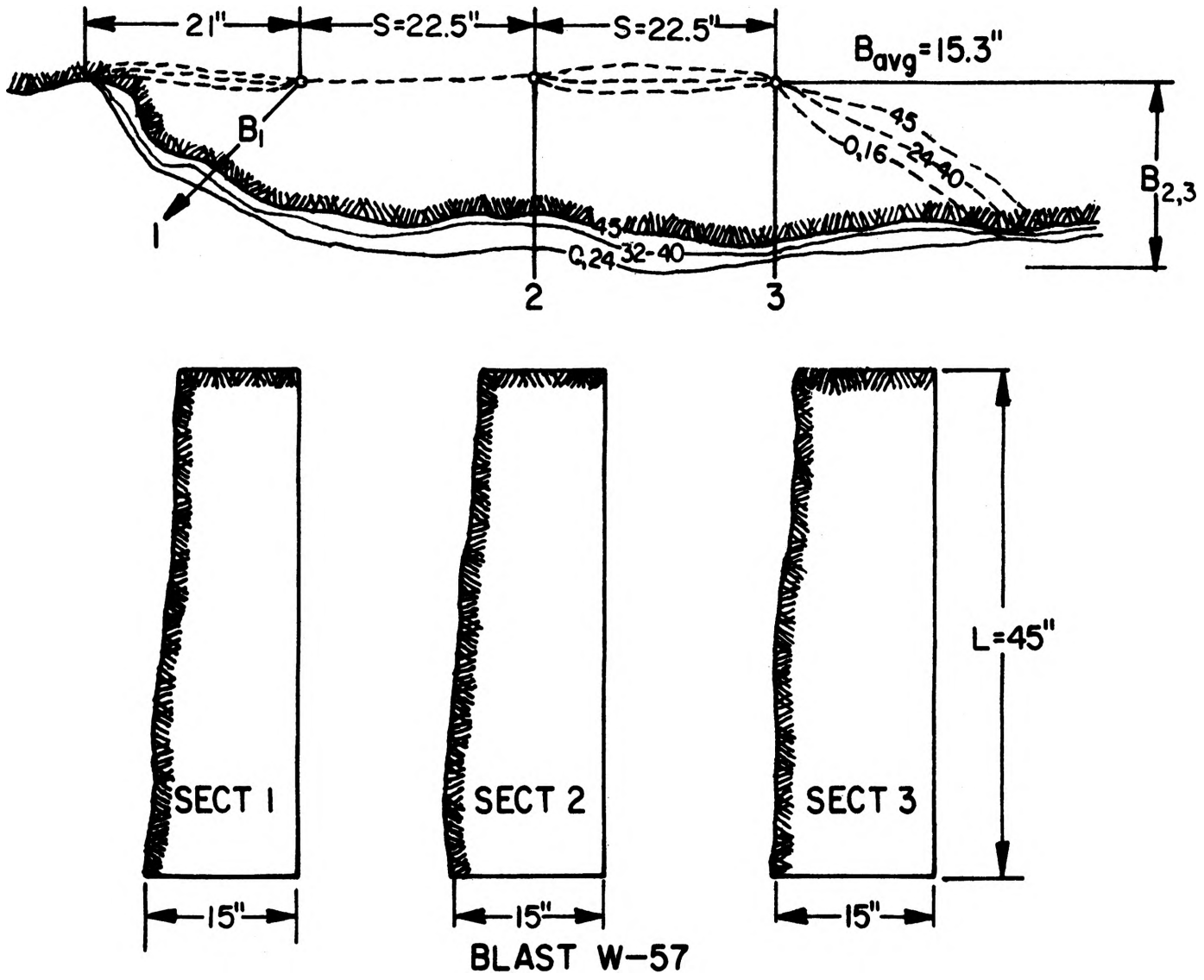

Figure E-6. Burden-Rock Contour Map and Vertical Sections for Test W-57.

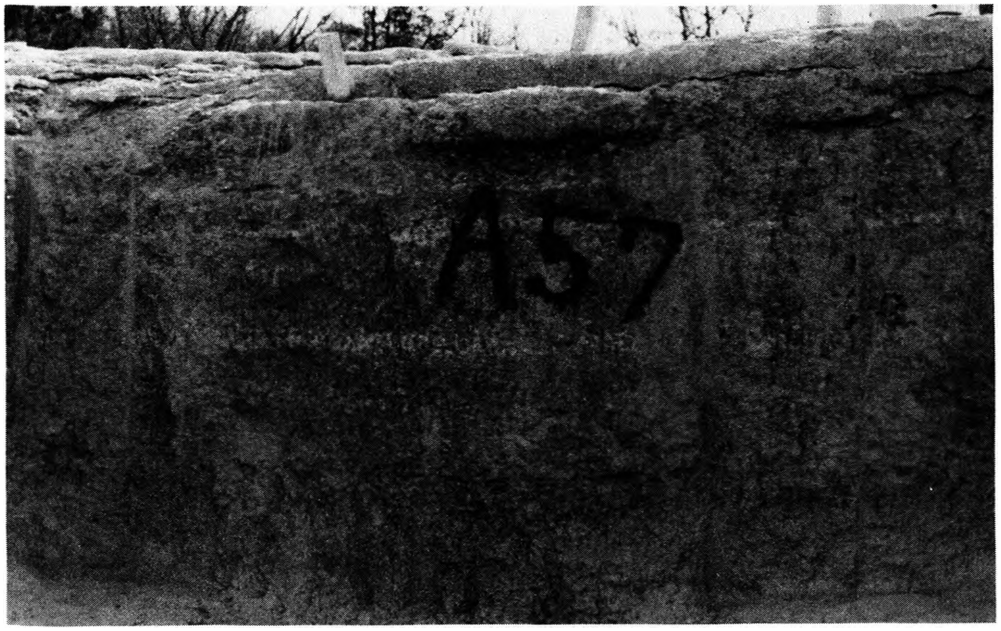

Figure E-7. Bench for Test A-57 Before Blasting.

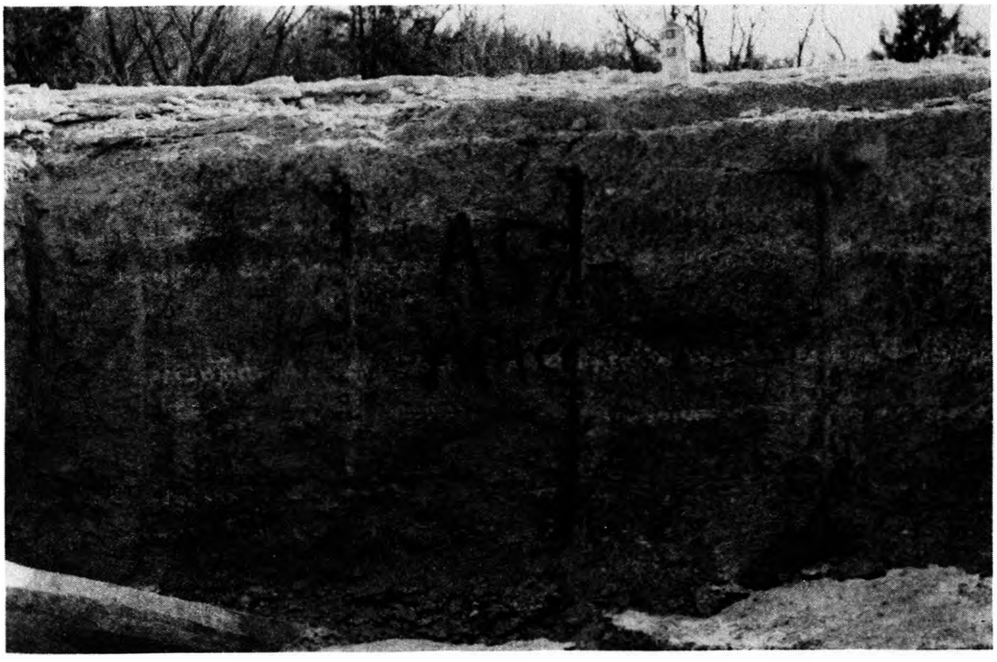

Figure E-8. Bench for Test A-57 After Blasting.

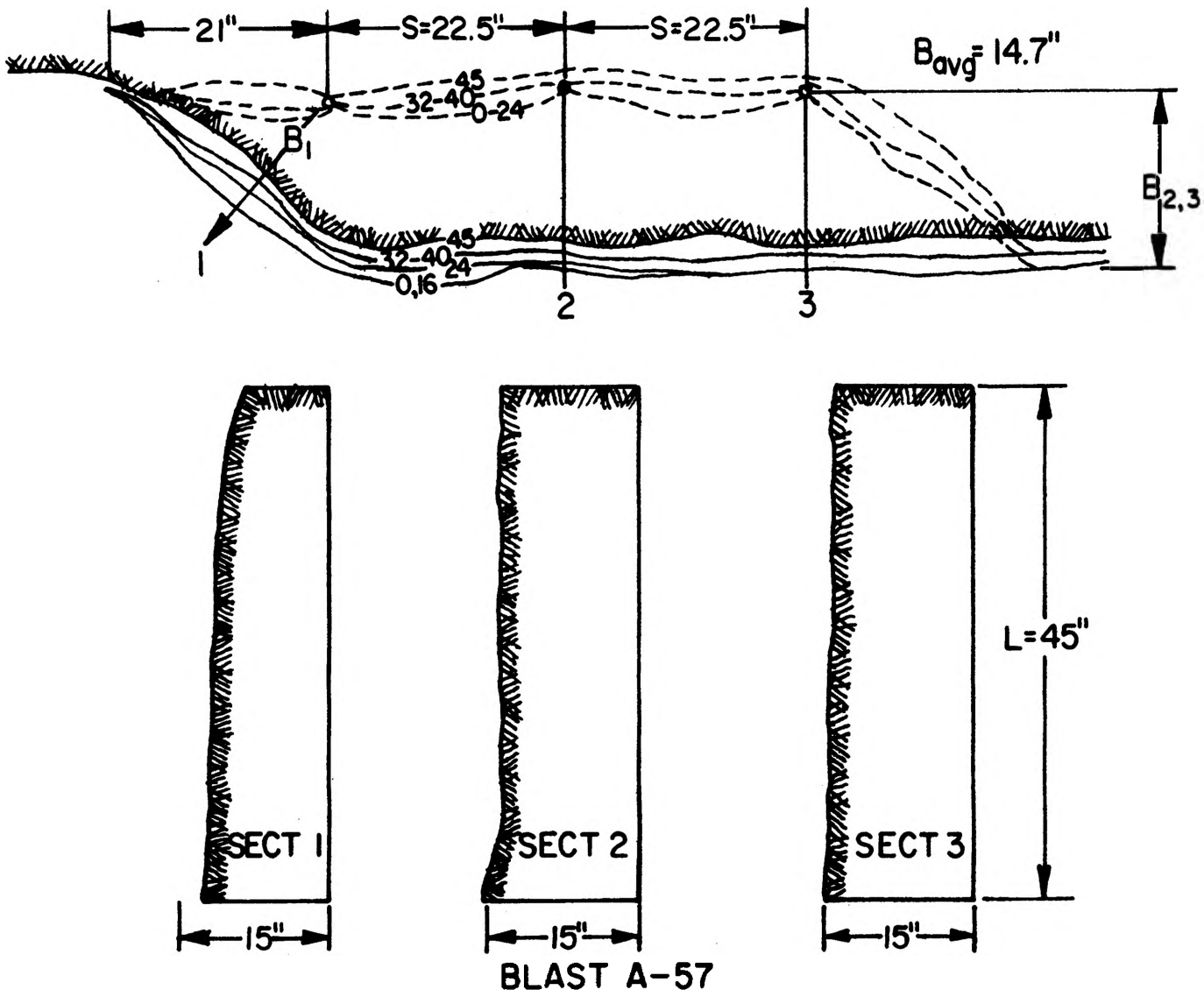

Figure E-9. Burden-Rock Contour Map and Vertical Sections for Test A-57.

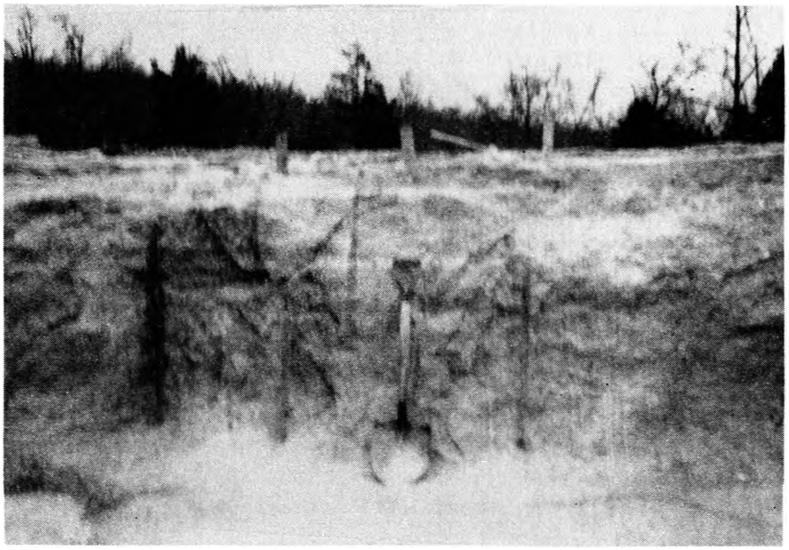

Figure E-10. Bench for Test A-47 Before Blasting.

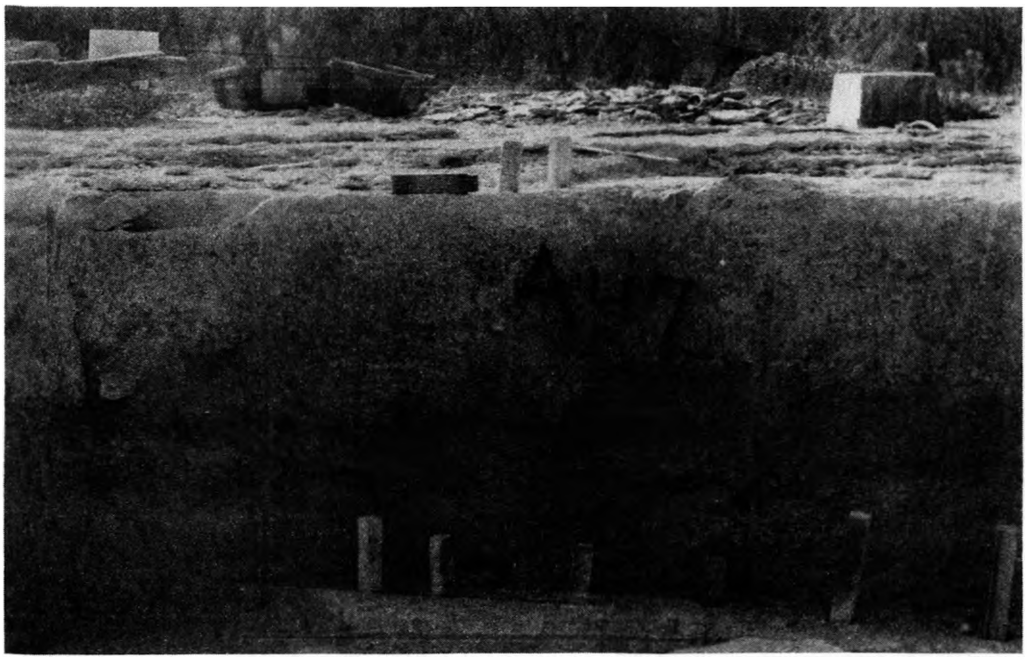

Figure E-11. Bench for Test A-47 After Blasting.

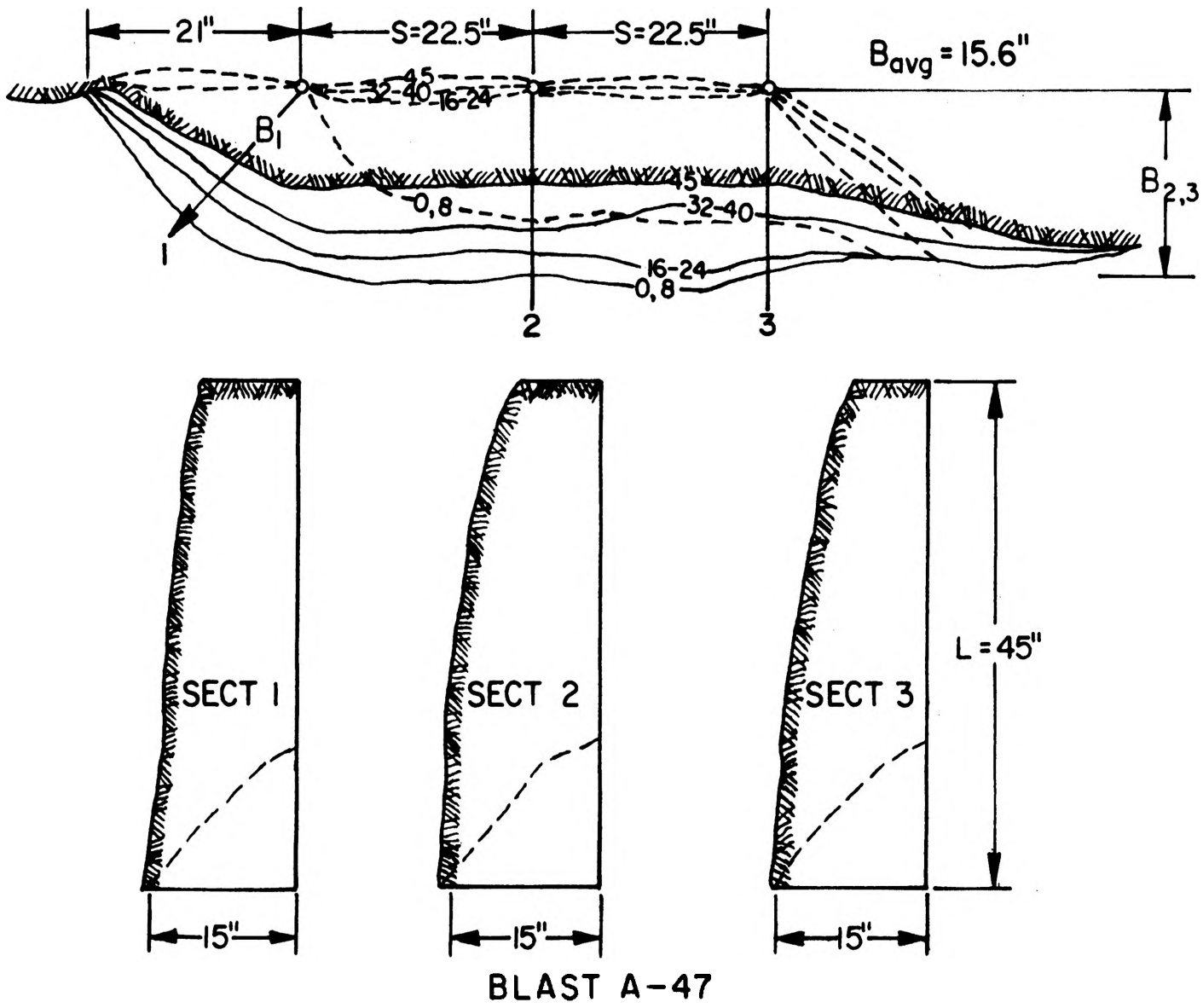

Figure E-12. Burden-Rock Contour Map and Vertical Sections for Test A-47.

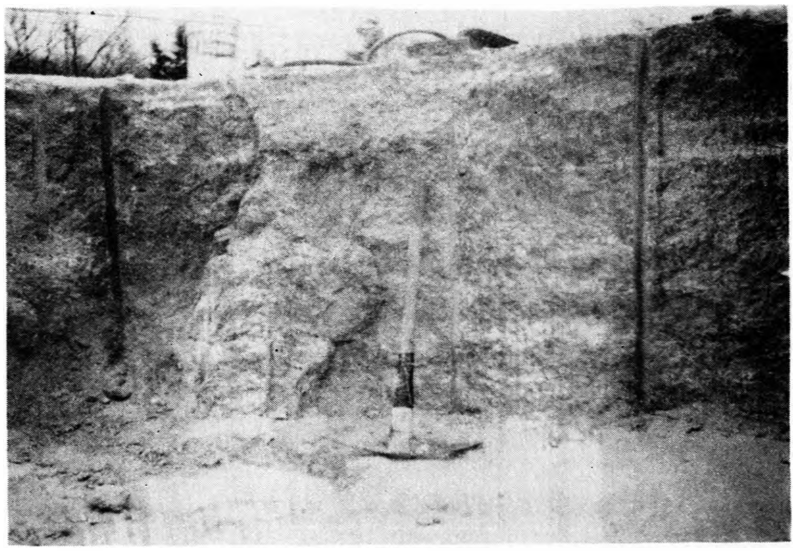

Figure E-13. Bench for Test W-40 Before Blasting.

Figure E-14. Bench for Test W-40 After Blasting.

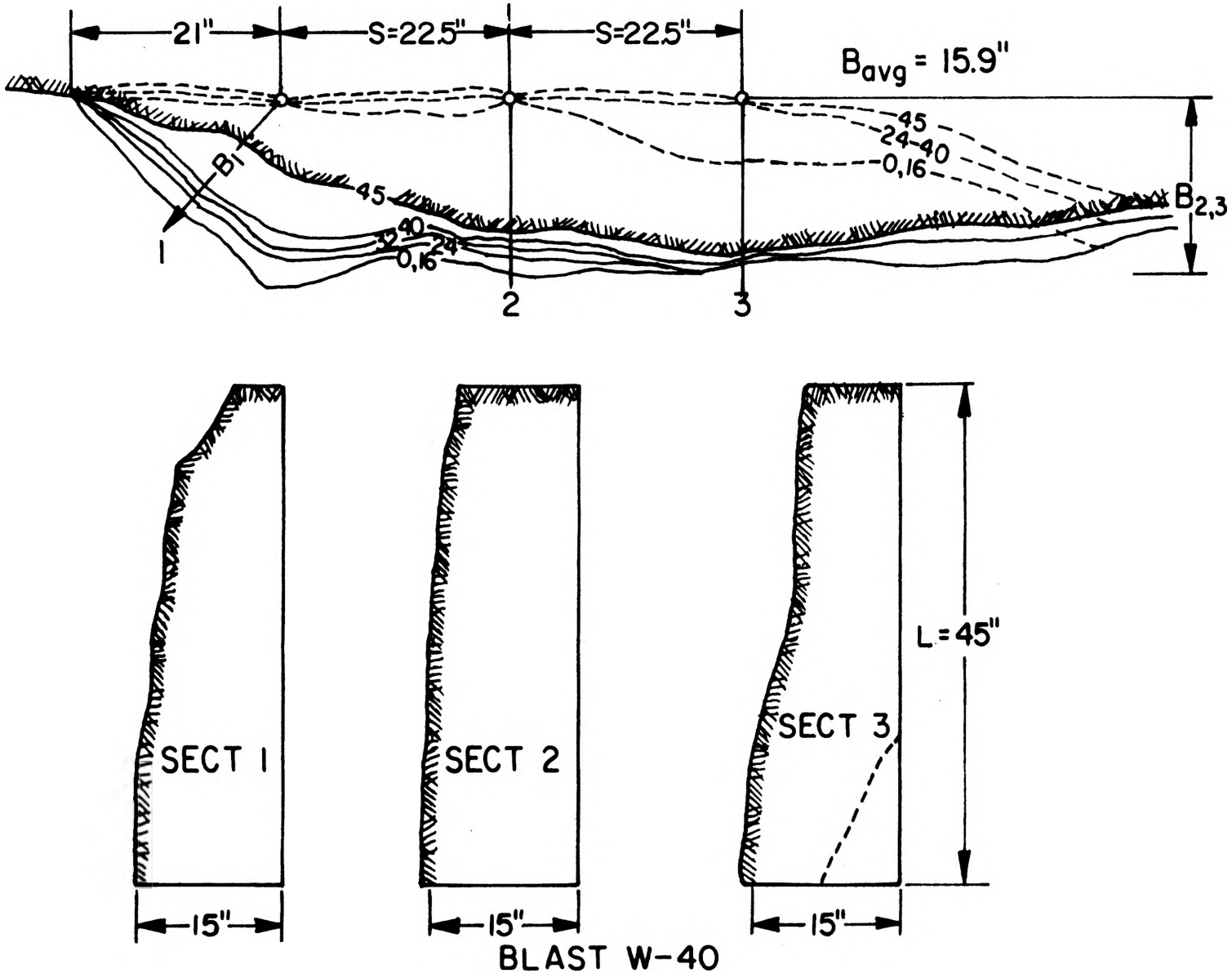

Figure E-15. Burden-Rock Contour Map and Vertical Sections for Test W-40.

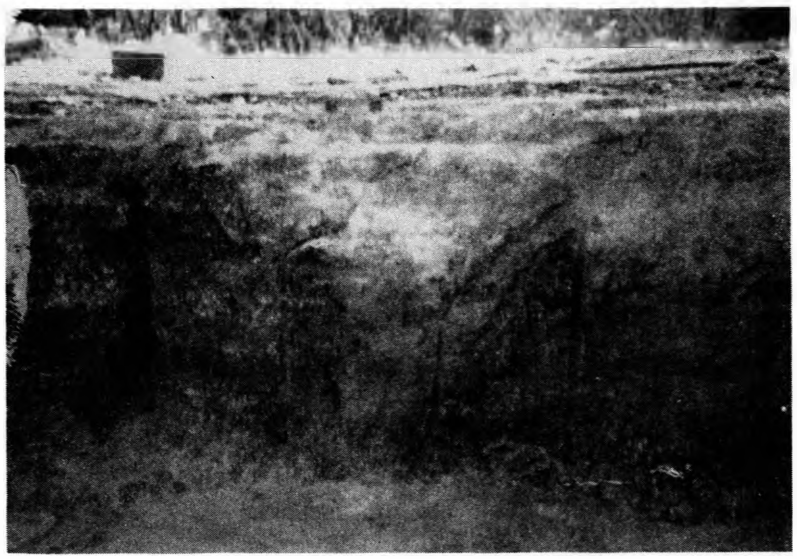

Figure E-16. Bench for Test A-40 Before Blasting.

Figure E-17. Bench for Test A-40 After Blasting.

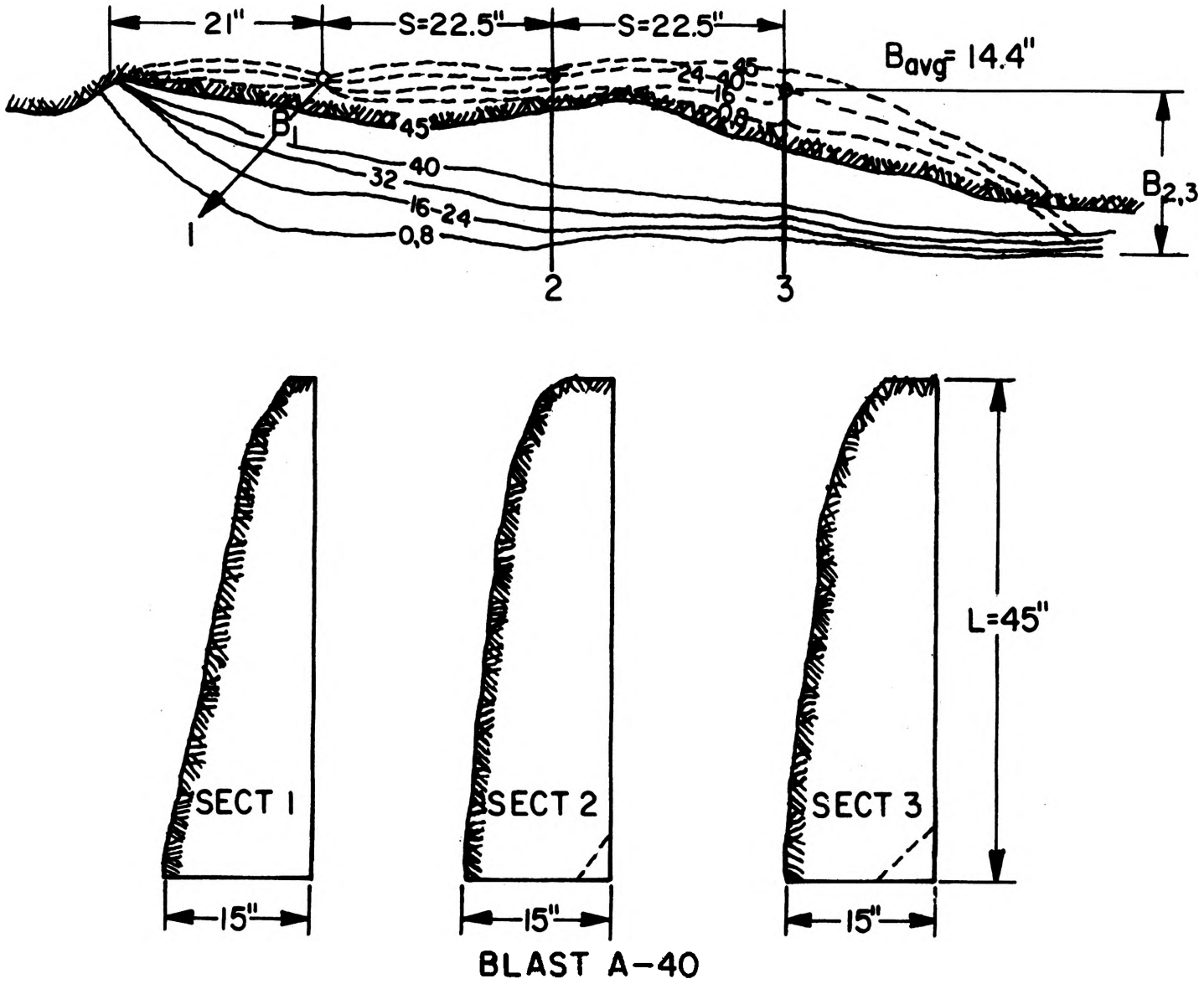

Figure E-18. Burden-Rock Contour Map and Vertical Sections for Test A-40.

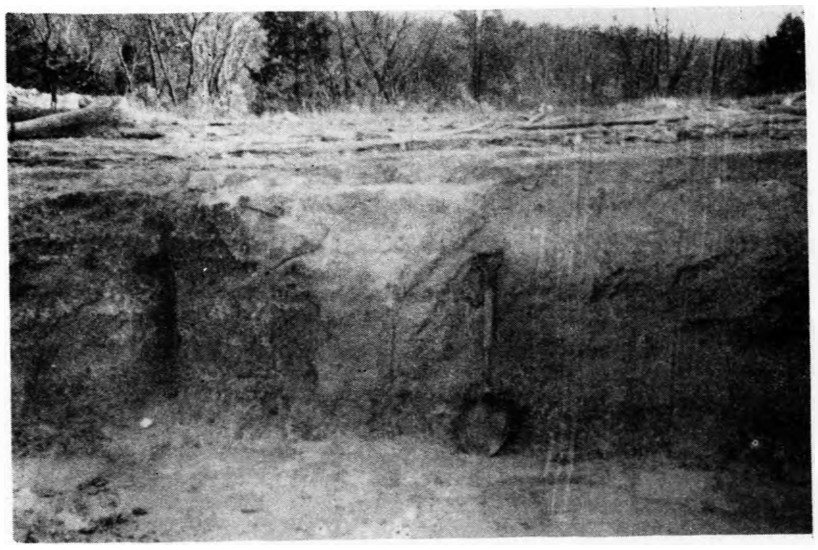

Figure E- 19. Bench for Test W-33 Before Blasting.

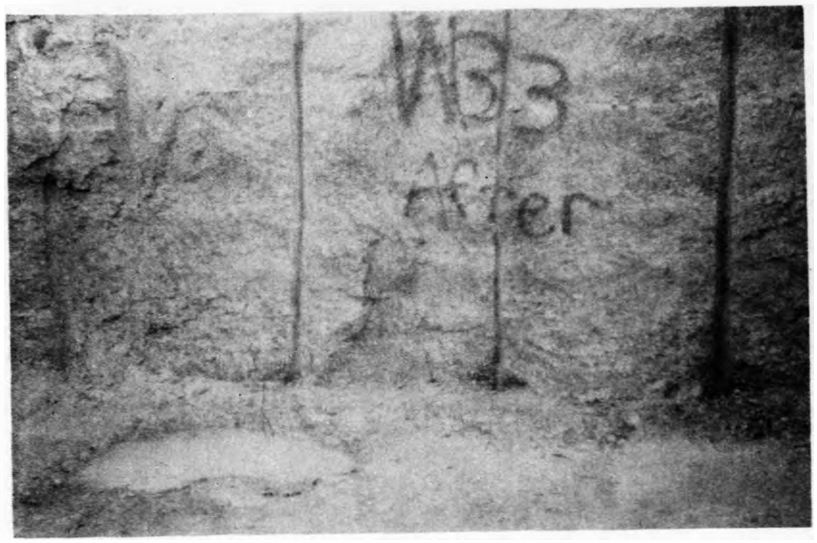

Figure E- 20. Bench for Test W-33 After Blasting.

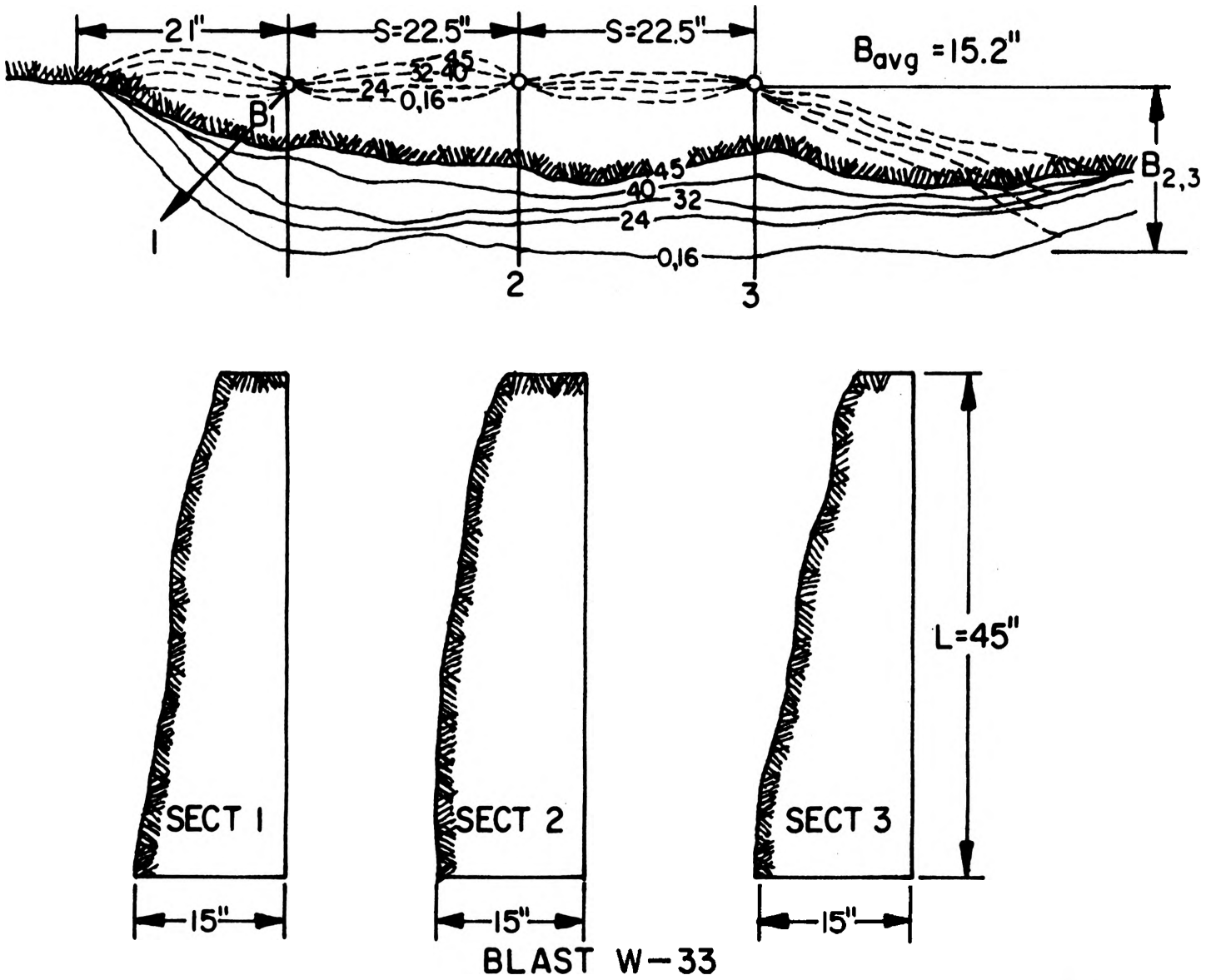

Figure E-21. Burden-Rock Contour Map and Vertical Sections for Test W-33.

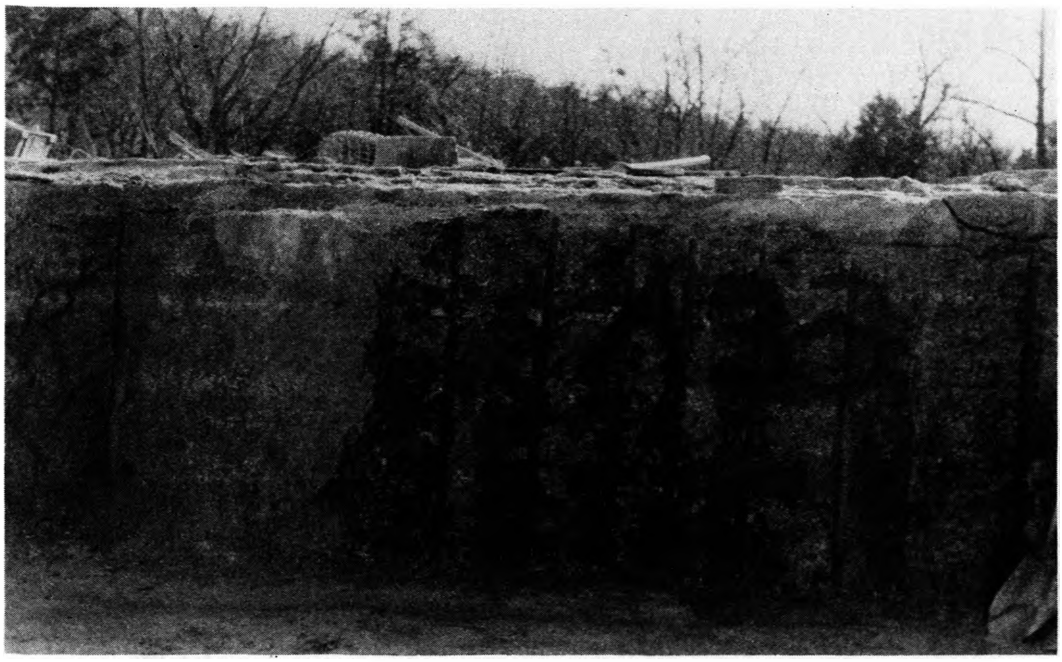

Figure E-22. Bench for Test A-33 Before Blasting.

Figure E-23. Bench for Test A-33 After Blasting.

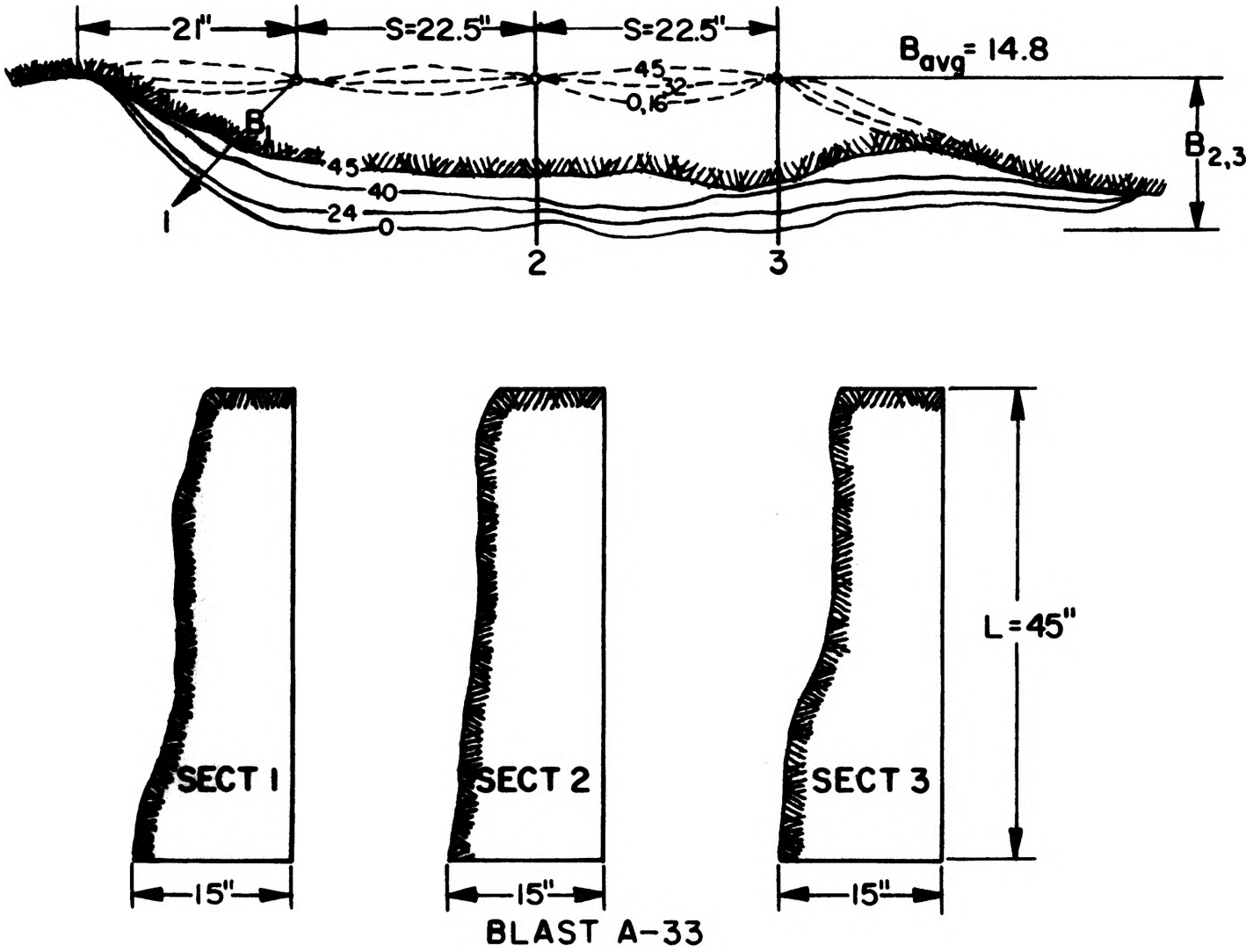

Figure E-24. Burden-Rock Contour Map and Vertical Sections for Test A-33.

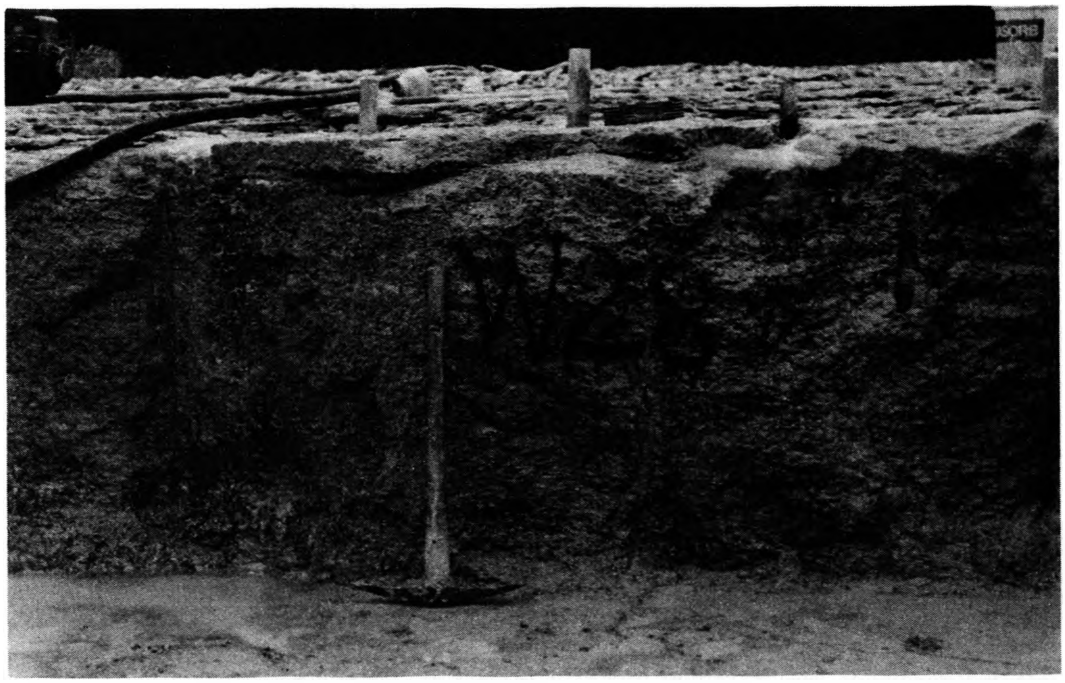

Figure E-25. Bench for Test W-28 Before Blastiing.

Figure E-26. Bench for Test W-28 After Blasting.

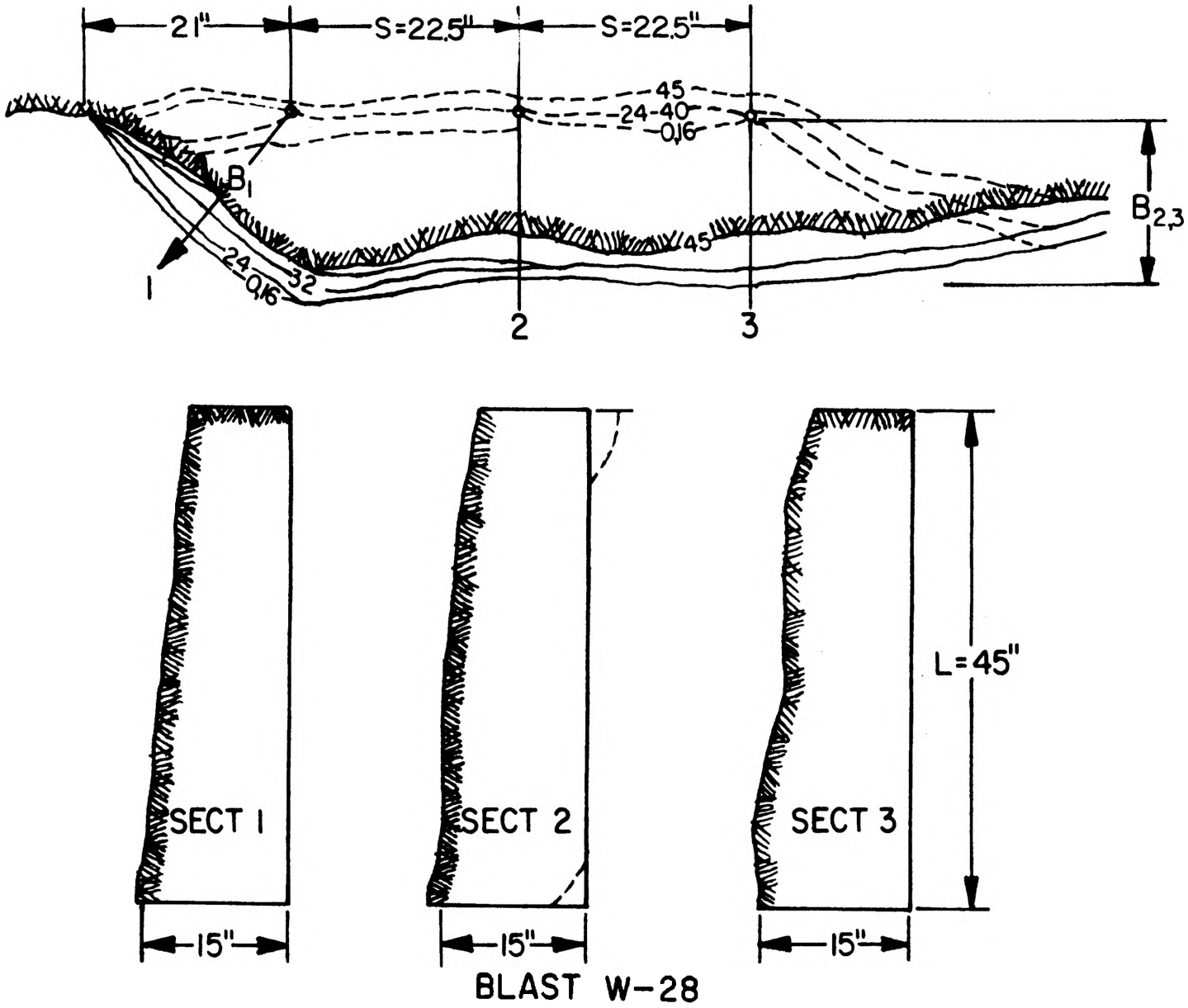

Figure E-27. Burden-Rock Contour Map and Vertical Sections for Test W-28.

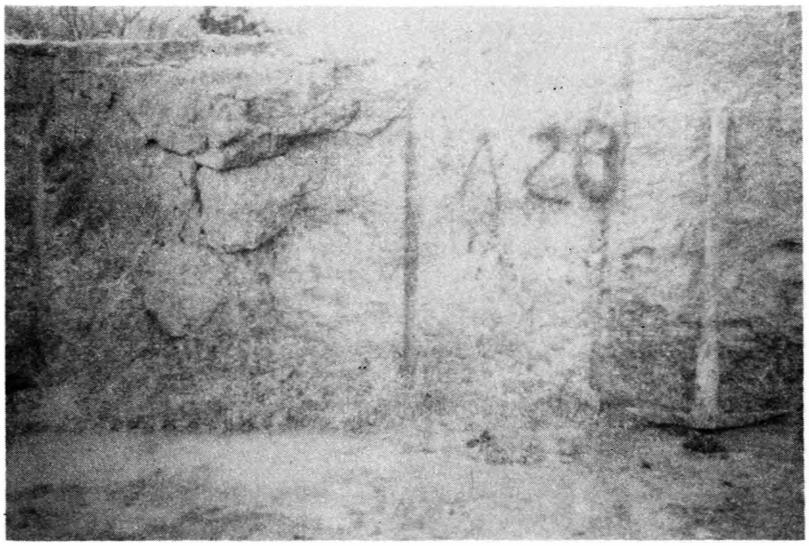

Figure E-28. Bench for Test A-28 Before Blasting.

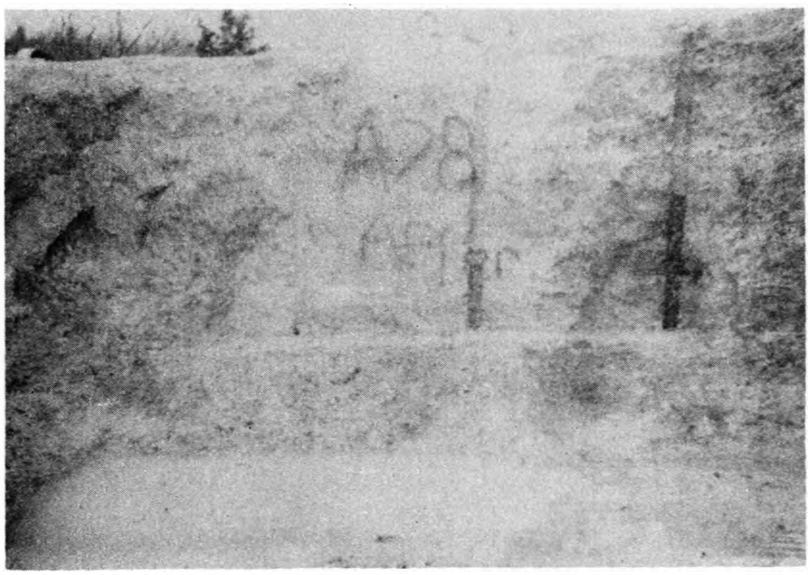

Figure E-29. Bench for Test A-28 After Blasting.

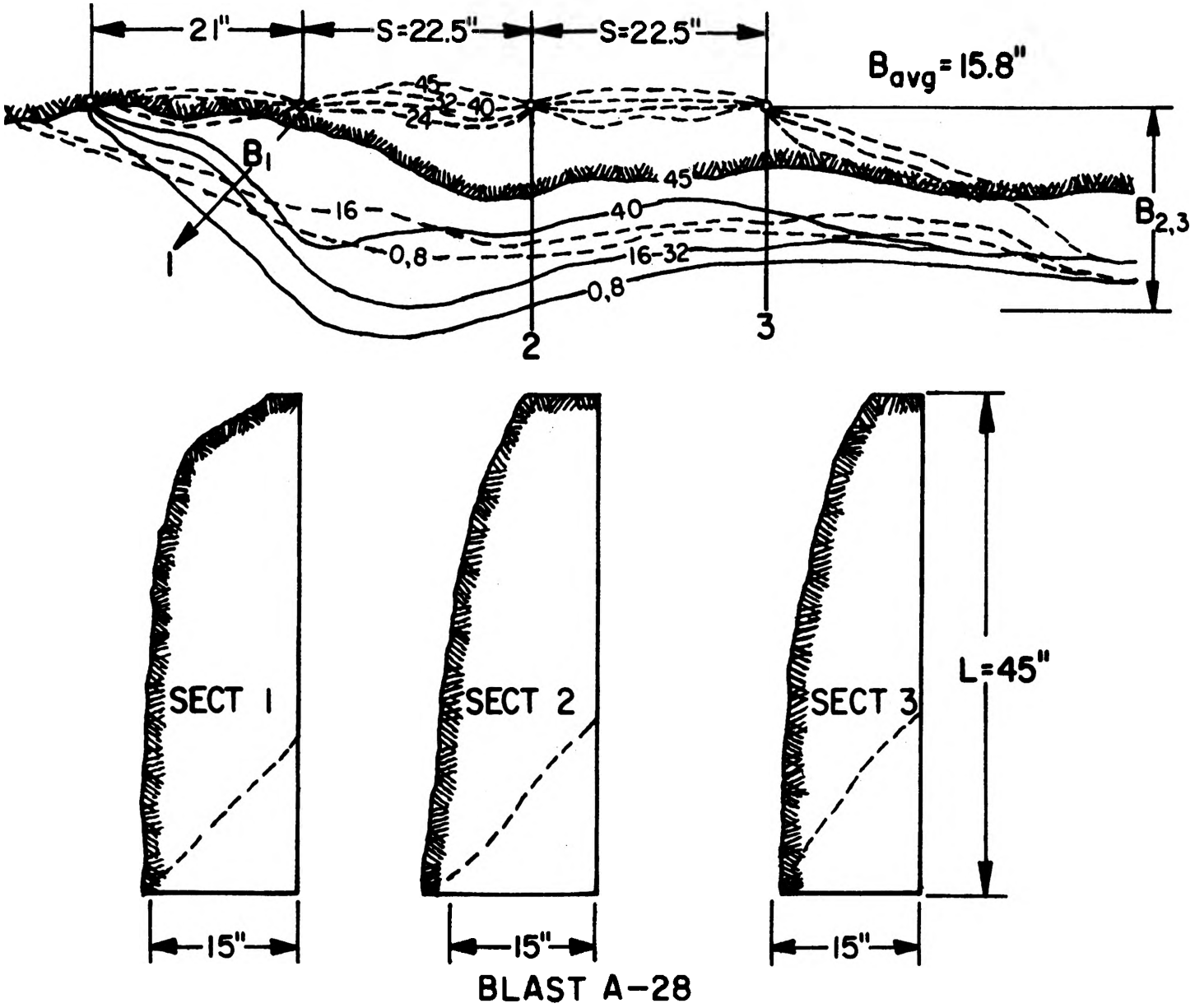

Figure E-30. Burden-Rock Contour Map and Vertical Sections for Test A-28.

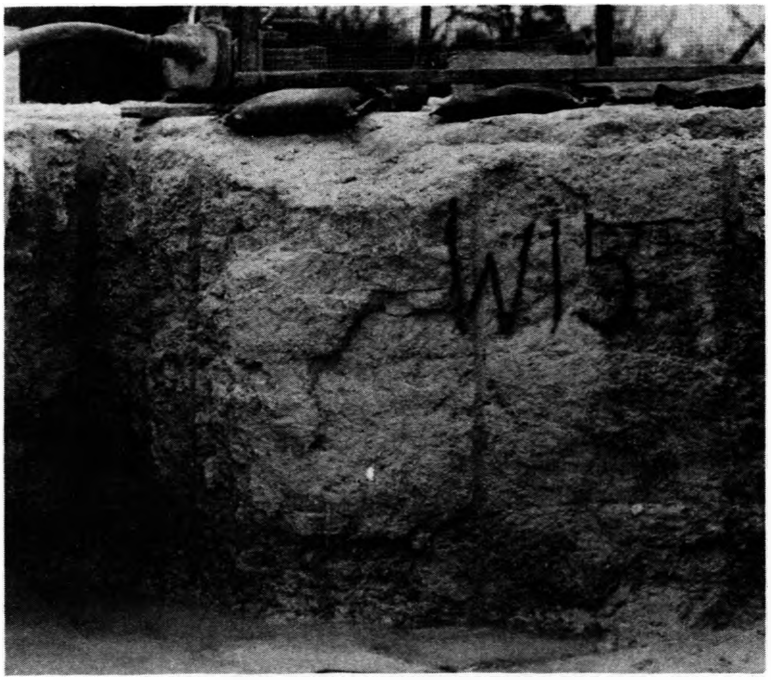

Figure E-31. Bench for Test W-15 Before Blasting.

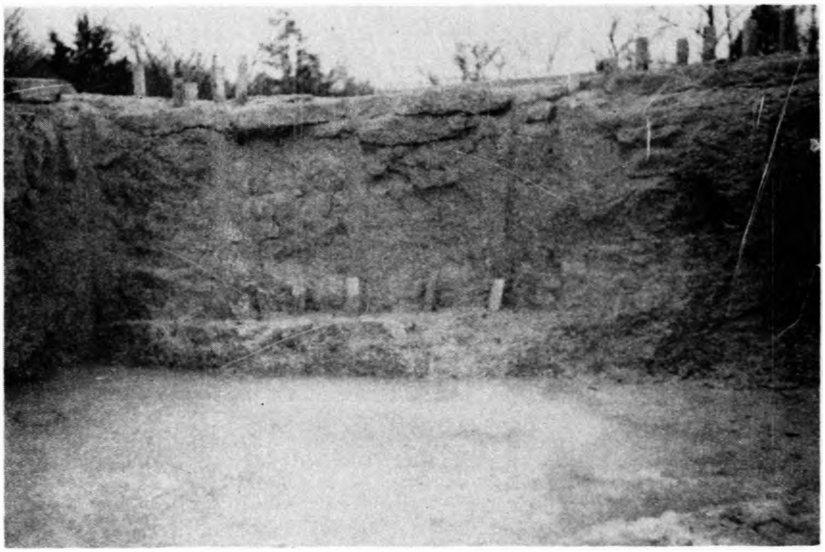

Figure E-32. Bench for Test W-15 After Blasting.

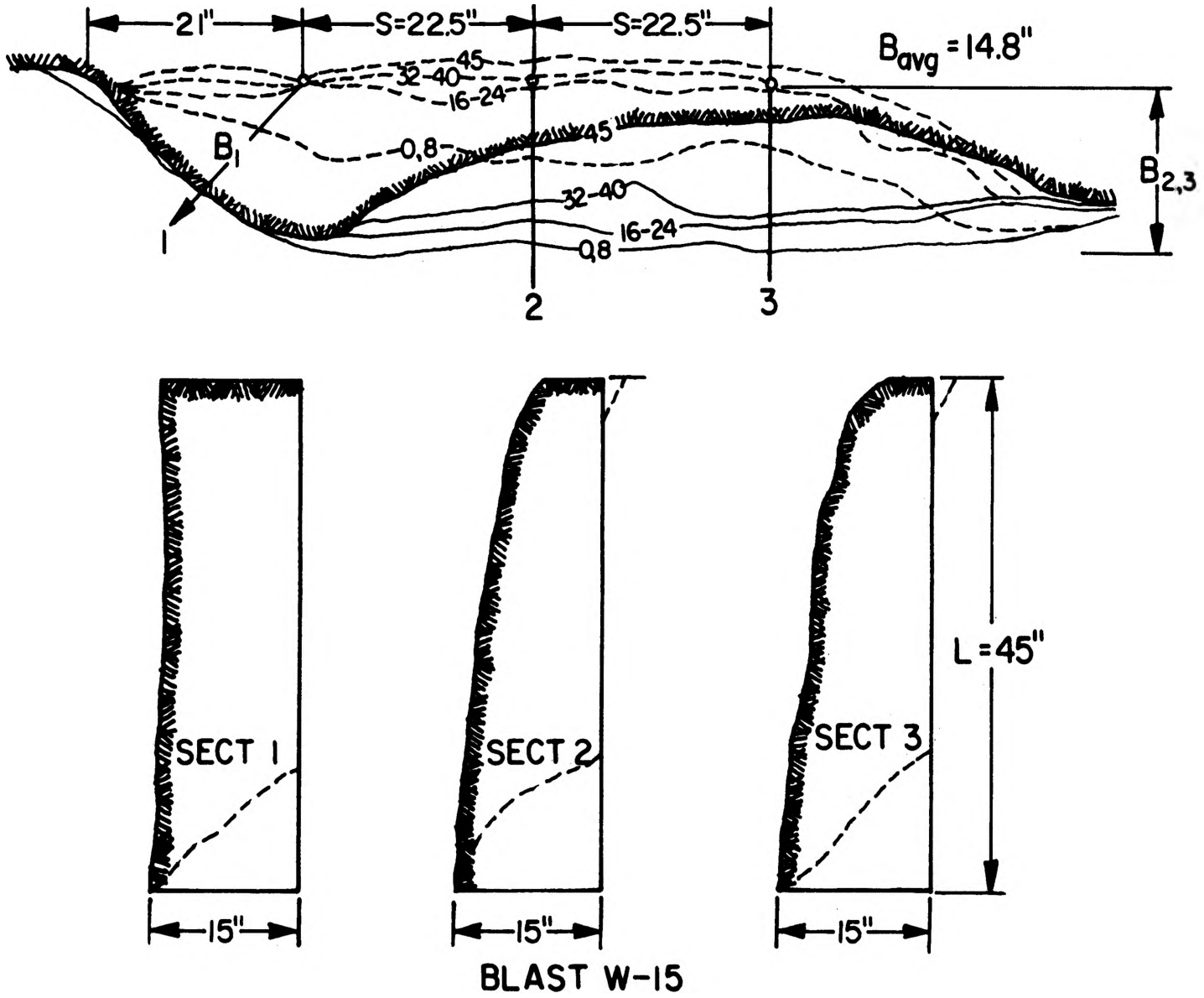

Figure E-33. Burden-Rock Contour Map and Vertical Sections for Test W-15.

APPENDIX F

RELATIONSHIP BETWEEN GEOMETRIC COUPLING AND WEIGHT PERCENT FOR INDIVIDUAL SIZE FRACTIONS

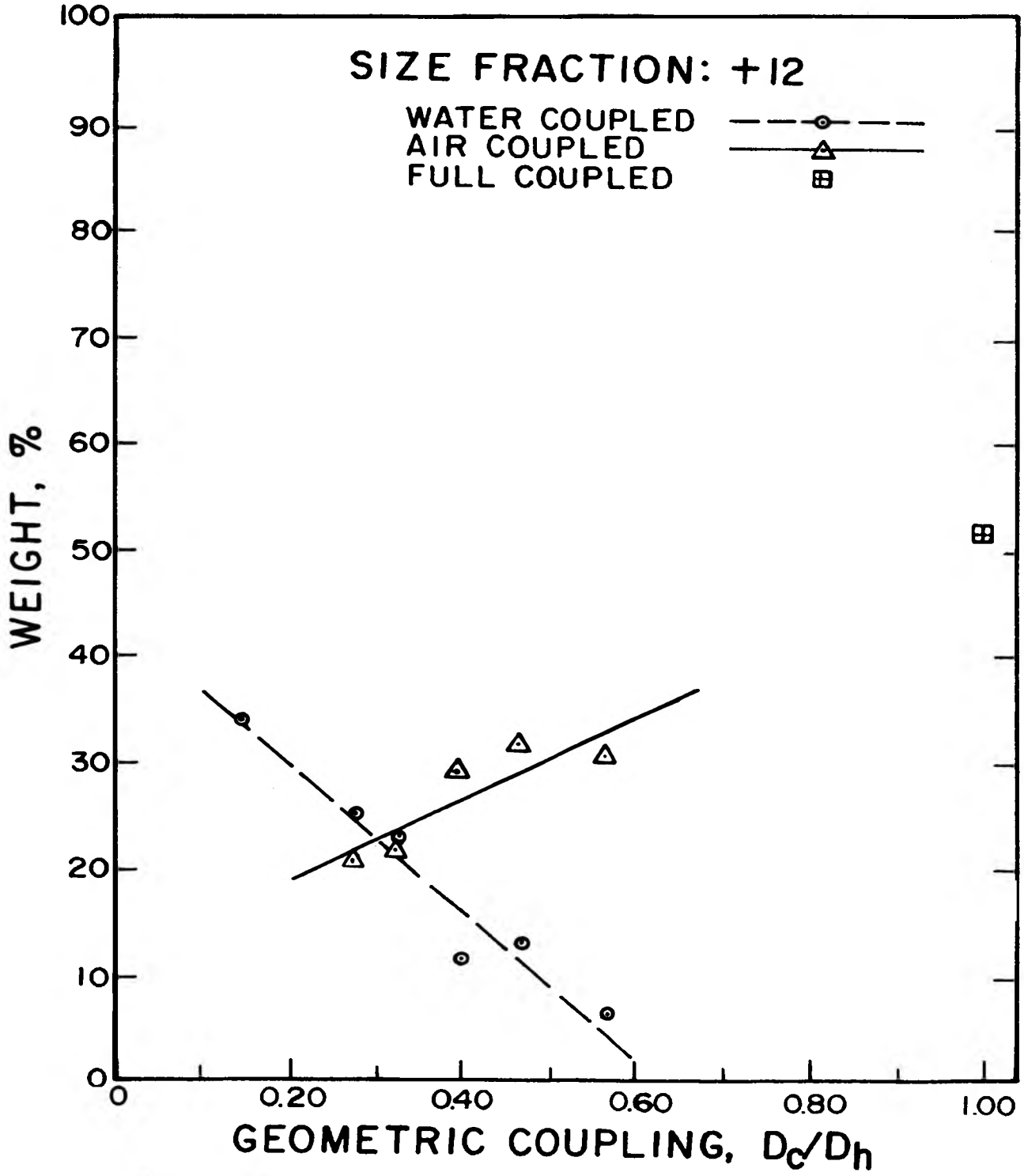

Figure F-1. Relationship Between Geometric Coupling and Weight Percents in the +12-inch Size-Fraction.

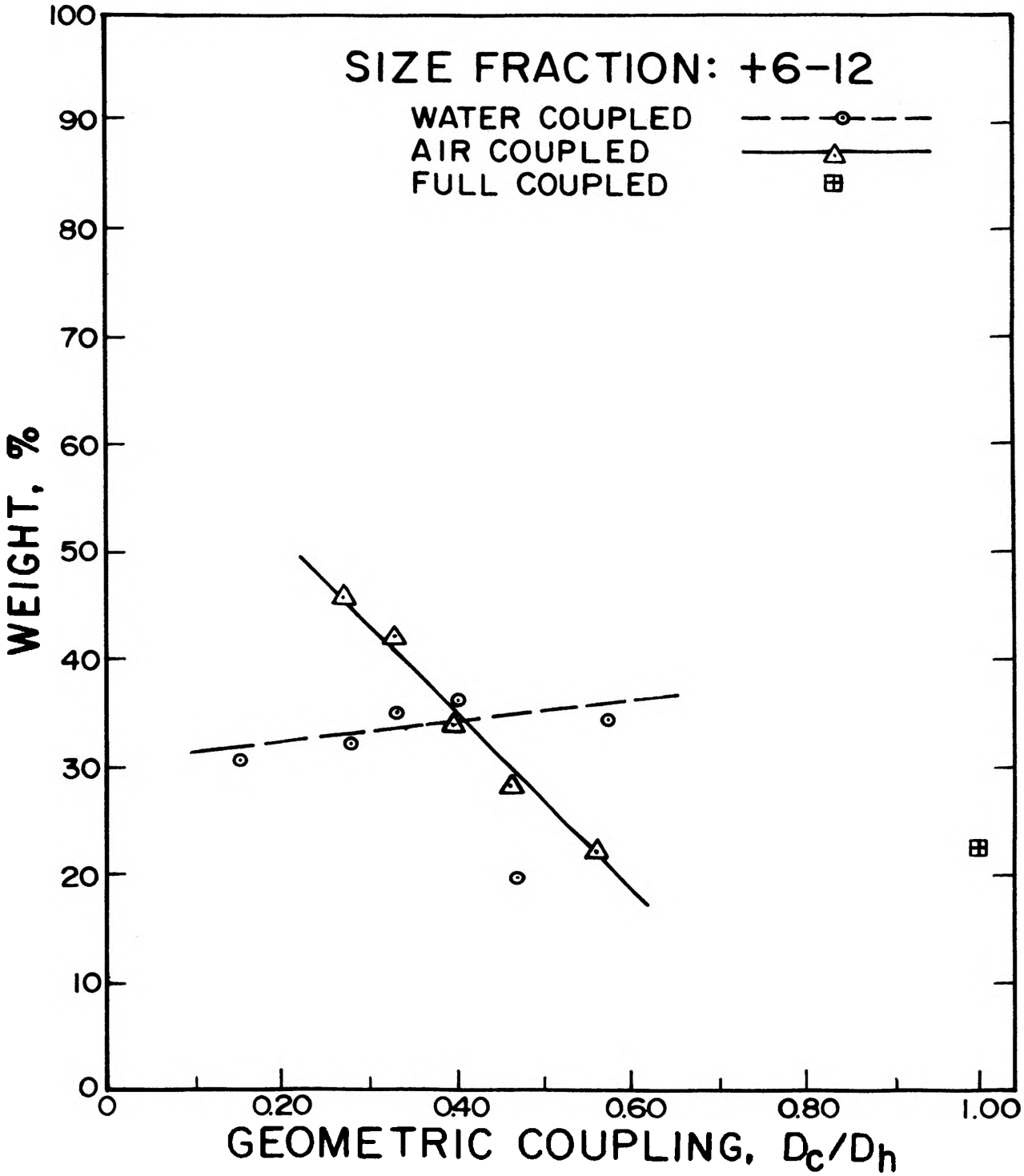

Figure F-2. Relationship Between Geometric Coupling and Weight Percents in the +6-12-inch Size-Fraction.

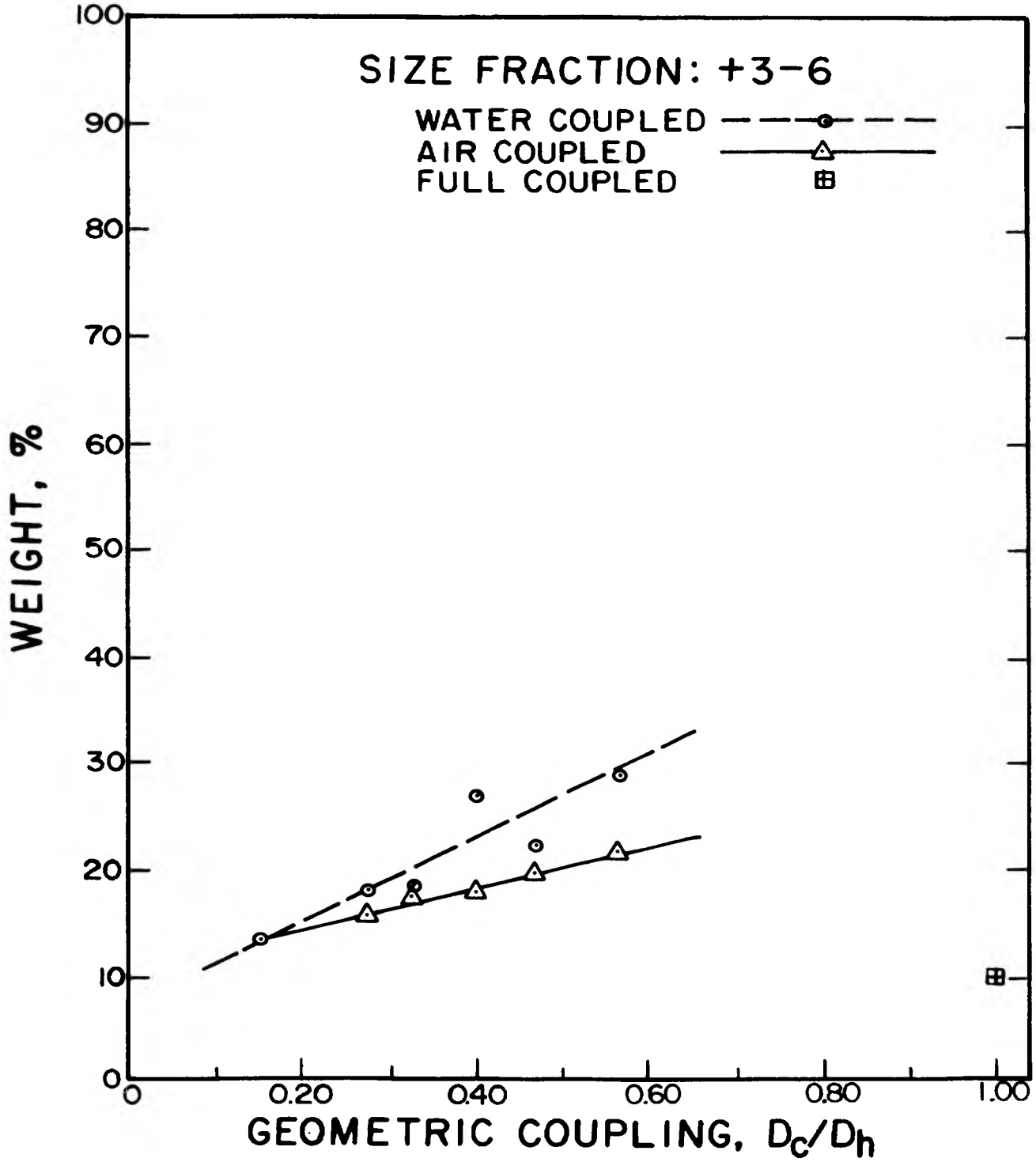

Figure F-3. Relationship Between Geometric Coupling and Weight Percents in the +3-6-inch Size-Fraction.

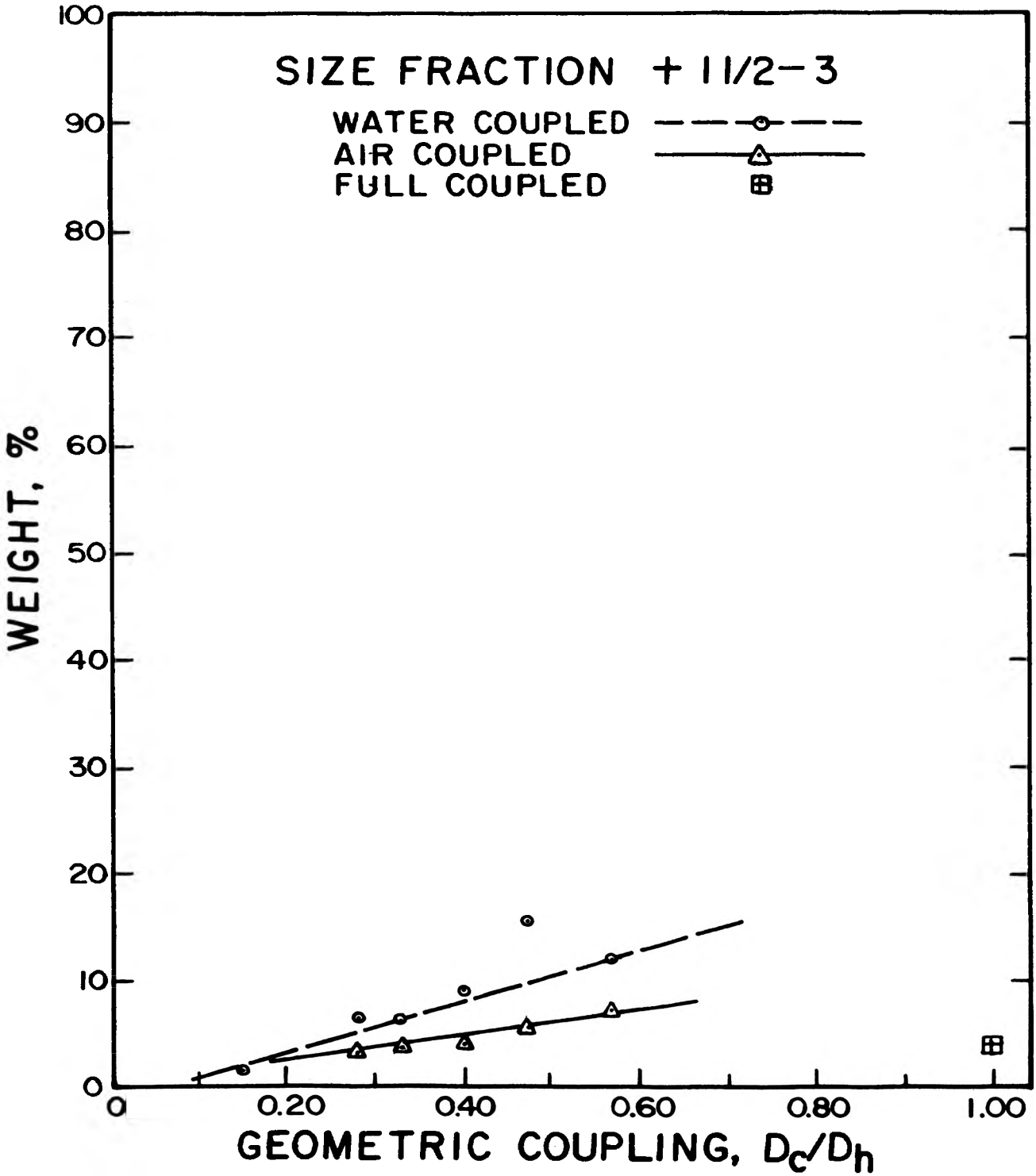

Figure F-4. Relationship Between Geometric Coupling and Weight Percents in the +1½-3-inch Size-Fraction.

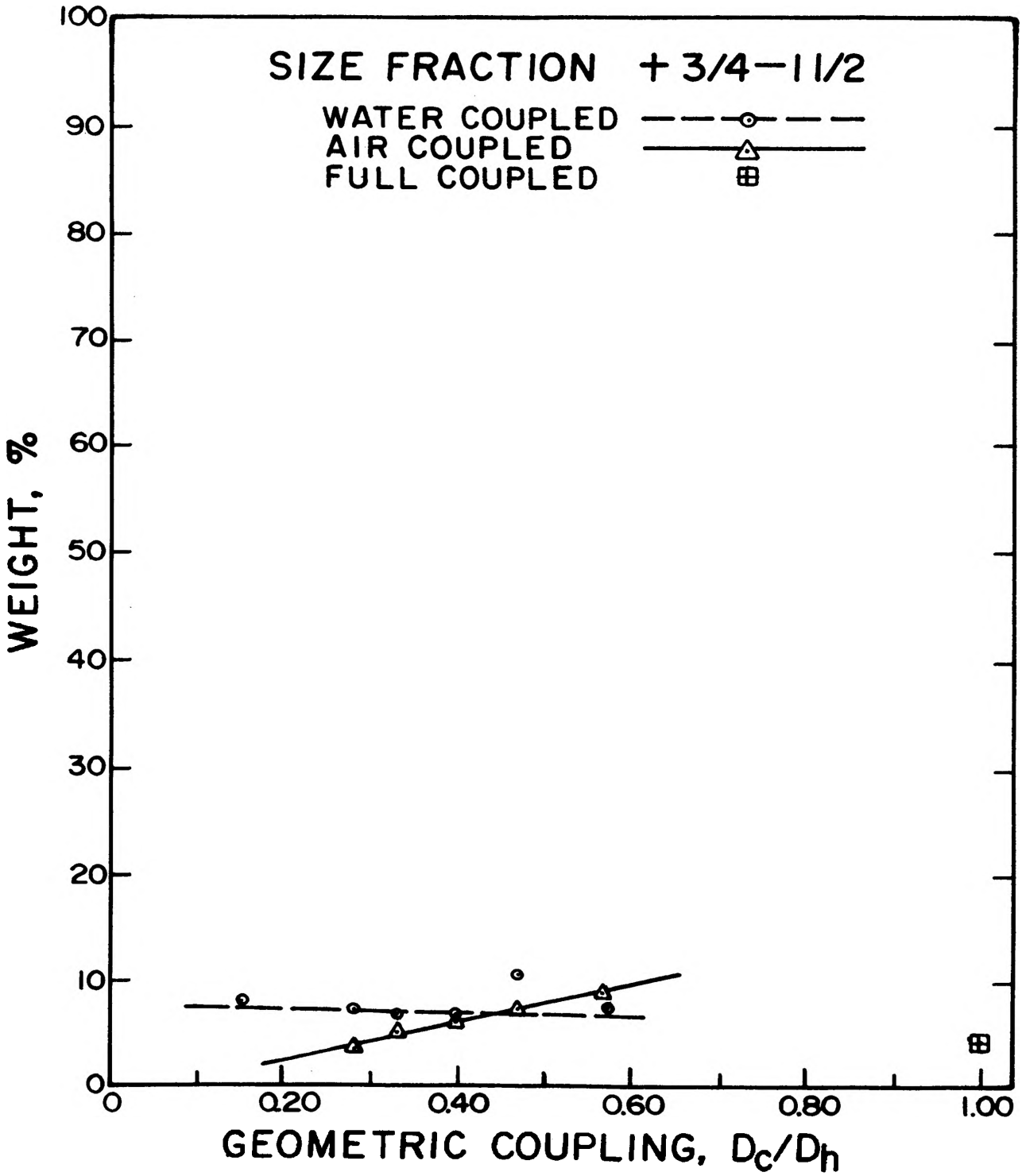

Figure F-5. Relationship Between Geometric Coupling and Weight Percents in the +3/4-1½-inch Size-Fraction.

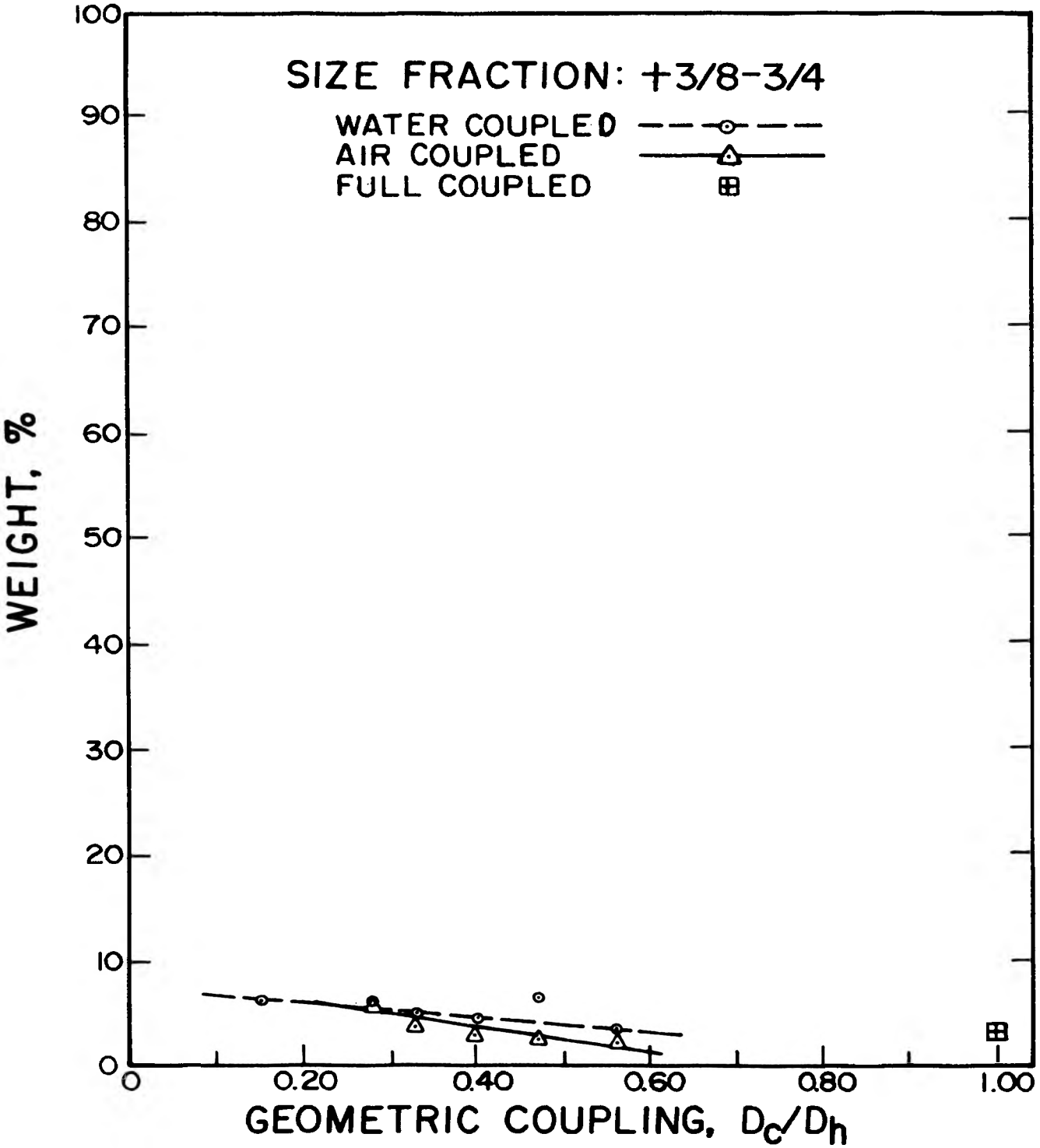

Figure F-6. Relationship Between Geometric Coupling and Weight Percents in the +3/8-3/4-inch Size-Fraction.

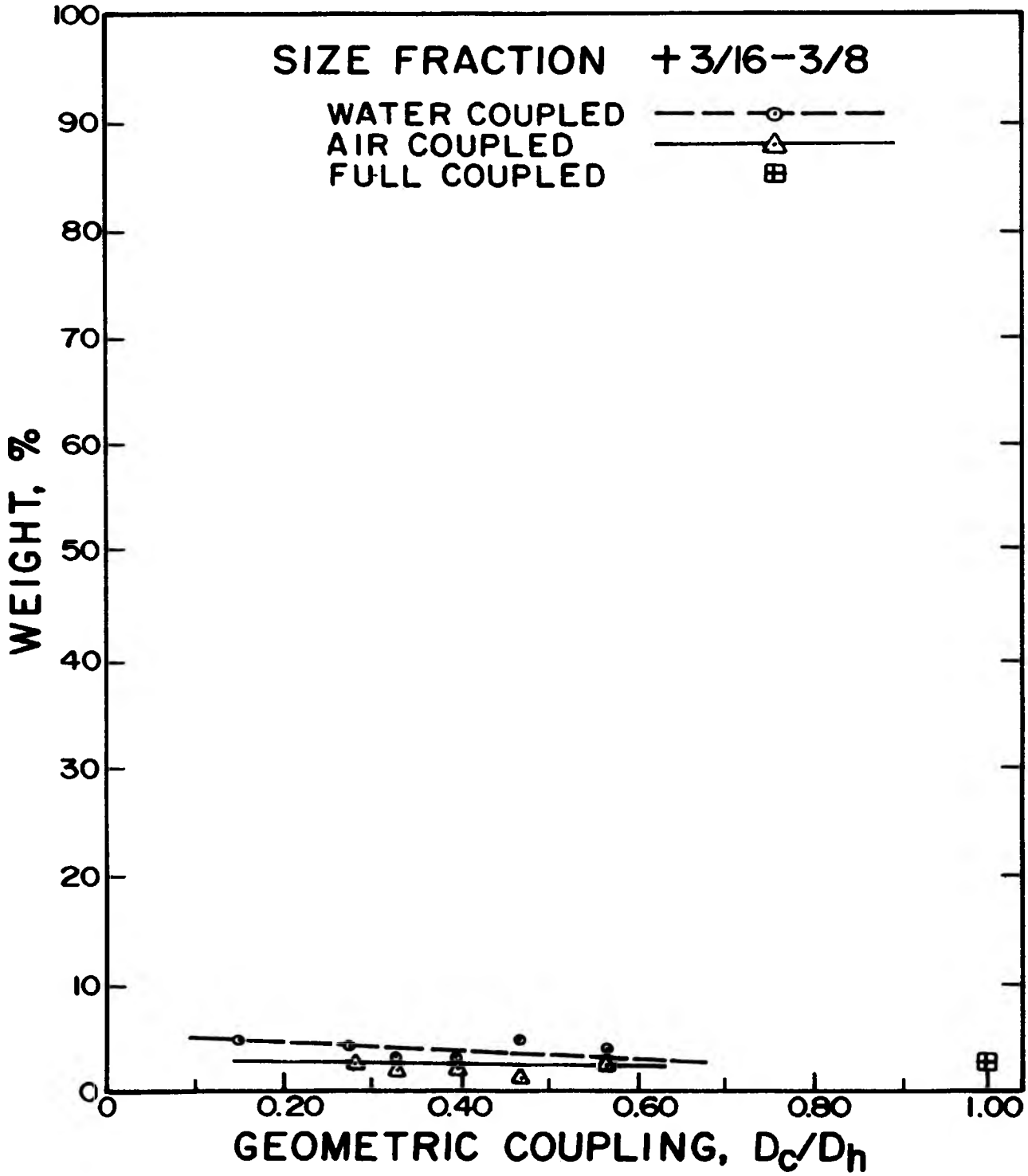

Figure F-7. Relationship Between Geometric Coupling and Weight Percents in the +3/16-3/8-inch Size-Fraction.

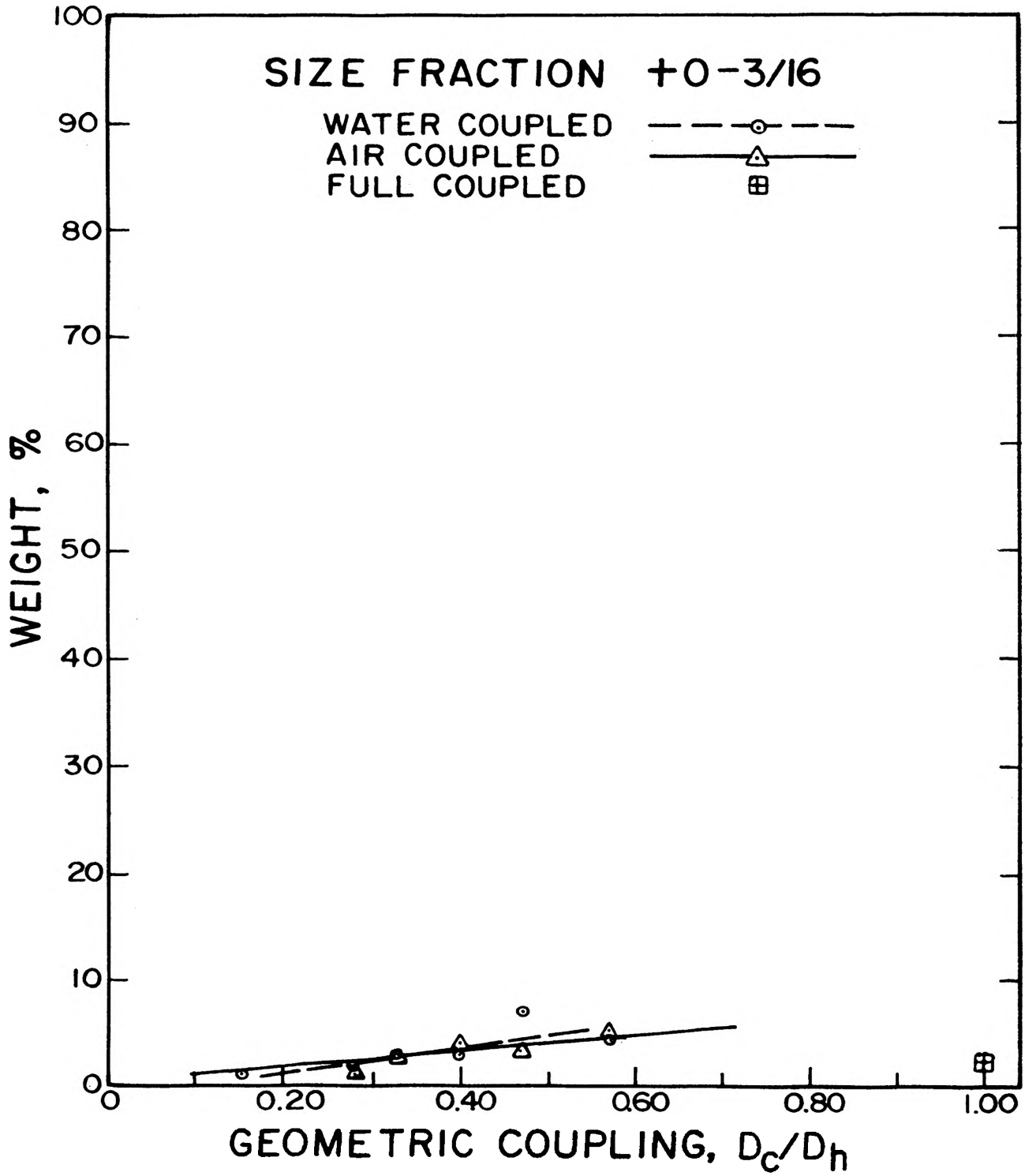

Figure F-8. Relationship Between Geometric Coupling and Weight Percents in the +0-3/16-inch Size-Fraction.

APPENDIX G

FRAGMENTATION INDICES AND SIZE RANGE PERCENTAGES FOR TEST BLASTS

TABLE G-I

FRAGMENTATION INDICES AND SIZE RANGE

PERCENTAGES FOR TEST BLASTS

Blast No.	Geometric Coupling	Coupling Medium	Cumulative Weight Percents			
			F_c	F_{+6}	$F_{+3/4-6}$	$F_{-3/4}$
F-1	1.00	Rock	0.791	74.2	18.0	7.8
A-57	0.57	Air	0.708	52.5	37.9	9.6
A-47	0.47	Air	0.738	60.0	32.5	7.5
A-40	0.40	Air	0.735	62.8	28.3	8.9
A-33	0.33	Air	0.732	64.2	26.7	9.1
A-28	0.28	Air	0.738	66.7	23.4	9.9
W-57	0.57	Water	0.655	41.1	47.3	11.6
W-40	0.40	Water	0.684	47.8	41.9	10.4
W-33	0.33	Water	0.713	58.2	31.0	10.8
W-28	0.28	Water	0.712	57.4	31.2	11.4
W-15	0.15	Water	0.734	64.8	23.1	12.1

APPENDIX H

ROCK YIELD, OVERBREAK, AND TOE RESULTS FOR TEST BLASTS

TABLE H-I

ROCK YIELD, OVERBREAK, AND TOE RESULTS FOR TEST BLASTS*

Blast No.	In Situ	Actual	Variance of Actual Weight from Design (Percent)	Percent of Design Weight: Back-break	End-break	Total Over-break	Toe
F-1	5318	6494	+51.4	+22.4	+26.2	+48.6	-10.7
W-57	4600	4129	-3.75	+ 4.2	+ 0.5	+ 4.7	- 0.0
W-40	3745	3328	-22.4	+ 1.8	+ 3.1	+ 4.9	- 1.9
W-33	5022	4480	+ 4.4	+ 4.1	+ 1.7	+ 5.8	- 2.4
W-28	4444	4027	- 6.1	+ 2.1	+ 3.4	+ 5.5	- 1.4
W-15	4598	4144	- 3.4	+ 0.8	+ 1.2	+ 2.0	-12.8
A-57	4963	4214	- 1.8	+ 1.5	+ 1.6	+ 3.1	- 2.1
A-47	4765	4141	- 3.5	+ 4.1	+ 3.1	+ 7.2	-14.2
A-40	4322	3778	-11.9	+ 0.4	+ 1.8	+ 2.2	- 0.7
A-33	4121	3570	-16.7	+ 2.8	+ 3.8	+ 6.6	- 1.7
A-28	4432	3304	-22.9	+ 1.3	+ 2.2	+ 2.5	-11.3

*Design weight = 4290 lbs. for all blasts.